6-3-1958

The Use of Electrical Resistance Strain Elements in Three-Dimensional Stress Analysis

Robert I. Brasier

ELECTRICAL RESISTANCE STRAIN ELEMENTS - BRASIER

NAME AND ADDRESS	DATE
KASSIM TARHINI U. of Toledo	April-07-1986

THE USE OF ELECTRICAL RESISTANCE STRAIN ELEMENTS IN THREE DIMENSIONAL STRESS ANALYSIS

By

Robert I. Brasier

A Thesis
Submitted in Partial Fulfillment of the
Requirements for the Degree of
Master of Science in Engineering

The University of New Mexico

1958

This thesis, directed and approved by the candidate's committee, has been accepted by the Graduate Committee of the University of New Mexico in partial fulfillment of the requirements for the degree of

MASTER OF SCIENCE

E F Castetter
DEAN

June 3, 1958
DATE

Thesis committee

R. C. Dove
CHAIRMAN

C. T. Grace

Edward C. Rightley

This thesis, directed and approved by the candidate's committee, has been accepted by the Graduate Committee of the University of New Mexico in partial fulfillment of the requirements for the degree of

MASTER OF SCIENCE

June 3, 1958

DATE

Thesis committee

CHAIRMAN

TABLE OF CONTENTS

LIST OF SYMBOLS

a	Distance, support to load, inches
c	Distance from neutral bending axis, inches
E_c	Modulus of elasticity in compression, psi
E_t	Modulus of elasticity in tension, psi
f	Photoelastic fringe value, lbs/in-fringe
F	Force, pounds
g	Gravitational acceleration, ft/sec^2
GF	Gage factor,
GF_r, GF_u, GF_l, GF_t	Rosette, uniaxial, longitudinal, transverse gage factor
I	Moment of inertia, inches^4
K_t	Stress concentration factor, $\frac{\sigma \text{ max.}}{\sigma \text{ nominal}}$
l	Length, inches
M	Bending moment, inch-pounds
P	Pressure, psig
P_i, P_o	Internal, external pressure
R	Electrical resistance, ohms
S	Stress, psi
S_l, S_t	Longitudinal, tangential stress
v	Velocity of sound, inches / sec
y	Deflection, inches
YP	Yield point, psi
ϵ	Strain, in / in
ν	Poissons ratio

ρ Weight per unit volume, lb / in^3

σ Stress, psi

I. INTRODUCTION

The increasing complexity of mechanical elements and the increasingly high performance demanded of them makes the job of stress analysis more and more difficult. In many applications the resulting increased size and weight makes "beefing up"the part in question an unacceptable solution. As the part and the manner of loading become more complex,a theoretical investigation of the stress distribution becomes increasingly difficult or impossible. Existing methods of stress analysis are frequently limited to the measurement of surface strains.

At present, there is only one method available for determining the stress distribution at interior points of solids. This method is the relatively difficult one of three dimensional photoelastic analysis. This method involves (1) the construction of an optically clear photoelastic model, (2) loading the model at elevated temperature, (3) freezing the stress pattern in place, (4) cutting the model into thin slices and finally, (5) a complete photoelastic analysis of each slice.

The purpose of this thesis is to present a new method of experimental stress analysis and to give the solution to a problem which has been handled by this method.

The increasing complexity of [illegible]

high performance demanded of new [illegible]

more difficult. In many applications [illegible]

makes "beefing up" the part in question [illegible]

and the manner of loading become [illegible]

of the stress distribution becomes [illegible]

Existing methods of stress analysis [illegible]

of surface strains.

At present, there is only [illegible]

distribution at interior points [illegible]

difficult one of these [illegible]

(1) the construction of [illegible]

the model at elevated temperature [illegible]

(4) cutting the model [illegible]

elastic analysis of each slice.

The purpose of this [illegible]

stress analysis and to give [illegible]

ied by this method.

II. SCOPE OF INVESTIGATION

This thesis is an investigation of a new method of experimental stress analysis.

The investigation consists of:

(1) Developing a technique for constructing electrical resistance strain elements and imbedding them in plastic models.

(2) Showing, by means of a photoelastic analysis, that the presence of the gage produces only negligible disturbances of the strain pattern within the model.

(3) Calibration of the strain elements to determine the accuracy obtainable with this new technique.

(4) Construction of a model of a thick wall pressure vessel and the application of this technique for determining the stress distribution within the model.

(5) Comparison of experimental data with a theoretical analysis of the model.

III. LITERATURE REVIEW

The value, and difficulty, of three dimensional stress analysis has long been recognized. At present, three dimensional photoelasticity is utilized as the only available tool for determining the stress distribution at interior points of solids. Matzdorff (1)* has worked with a polyester resin called Castolite as a photoelastic material. Frocht (2) has reported on the use of Castolite for three dimensional photoelasticity and pointed out that Castolite has the useful property of bonding to itself to make a continuous, unstrained joint. He demonstrated this by means of photoelastic analysis.

Loh (3), among others, has constructed strain gages suitable for imbedding in masses of concrete. He points out the difficulty of constructing a gage with a suitable modulus and which "will serve to measure both tension and compression with a very high degree of accuracy". The Baldwin-Lima-Hamilton corporation now markets a gage designed for imbedding in concrete.

Dove (4) discussed the reinforcing effect of bonded wire strain gages on materials of low modulus. He reported an experiment which showed that the stiffening effect of the wire grid is only about 10% that of a type A-5-1 bonded wire strain gage. Dietz and Campbell (5) reported on the use of bonded wire gages on polymethyl methacrylate specimens. They stated that values of modulus obtained from strain gage data agreed well with those

---

* Numerals in parenthesis refer to corresponding items under the heading, "LITERATURE CITED".

[illegible]

The value, [illegible] long been recognized. [illegible] utilized as the only available [illegible] at interior points of [illegible] resin called Castolite as a [illegible] on the use of Castolite for [illegible] out that Castolite has the [illegible] continuous, unstrained [illegible] analysis.

Lon (3), among others, has [illegible] imbedding in masses of [illegible] a gage with a suitable [illegible] and compression with a very [illegible] Hamilton corporation [illegible]

Dove (4) discussed the [illegible] on materials of low modulus [illegible] the stiffening effect of [illegible] Ar-1 bonded wire strain [illegible] of bonded wire gages on polyester [illegible] values of modulus obtained [illegible]

---

* Numerals in parentheses refer to [illegible] heading, "LITERATURE CITED".

obtained by other methods. However, Eney (6) pointed out the possibility of a stiffening effect caused by the gages. Clark (7) used bonded wire strain gages in conjunction with CR-39 photoelastic models and demonstrated that the gages not only gave only 75% of the actual strain but also influenced the stress distribution. Gerard and Gilbert (8) were successful in imbedding thermocouple wires in photoelastic models with practically no effect on the stress distribution.

In the present investigation, material on the analysis of thick wall pressure vessels was taken from Murphy (9) and two dimensional stress concentration factors from Peterson (10). Information on strain gages and gage application was obtained from Perry and Lissner (11) and Lee (12). Lee also gives information on photoelastic analysis which was used for determining the effect of the imbedded strain elements. Meier (13) shows methods of determining the gage factor of the strain gages and Dohrenwend and Mehaffey (14) give suggestions on the calibration of the gages.

The author knows of no work in which electrical resistance strain elements have been imbedded in plastic models as a three dimensional stress analysis technique.

determining the effect of [illegible]

methods of determining [illegible]

and Mehaffey (14) give [illegible]

The author knows of no [illegible]

elements have been [illegible]

analysis technique.

IV. CONSTRUCTION OF ELECTRICAL RESISTANCE STRAIN ELEMENTS

The electrical resistance strain elements used in this work consist of approximately 4.9" of 0.001" diameter gage wire soldered between two 0.004" diameter tinned copper lead wires. This wire is wound around a 0.010" thick wafer of Castolite plastic, and cemented in place. The gage wire used is a 55% copper, 45% nickel alloy "Advance" manufactured by the Driver Harris Corporation, Harrison, New Jersey. The lead wires were soldered using a 25 watt soldering iron with a tapered, ¼" diameter tip. Ninety-five volts were applied to the iron. 0.095" diameter Kester rosin core solder was used with Nokorode soldering paste. The soldering paste should be used sparingly. Figure 1 shows a jig used in winding the wire element on its plastic backing. Each gage should be wound under the same uniform tension, for reproducibility. In this case a no. 3/0 split shot (weight 0.8 gm.) was attached to an additional length of 0.001" diameter wire and looped ever the gage wire during the winding operation. Additional castolite plastic was used for a cement. Castolite is the trade name of a polyester casting resin made by the Castolite company Woodstock, Illinois. When the cement has hardened the gage is ready to imbed in the model. Figure 2 is a sketch of a gage made by this method. Directions for casting and curing the Castolite resin are given in the appendix. It was found, that when the resin was to be used in a very thin section such as coating a gage element or bonding other pieces together, twice the recommended amount of catalyst could be used. The catalyst supplied by the Castolite company was not suitable for this work since it resulted in a highly stressed casting. The Hercules Powder Company's 72.2% concentration

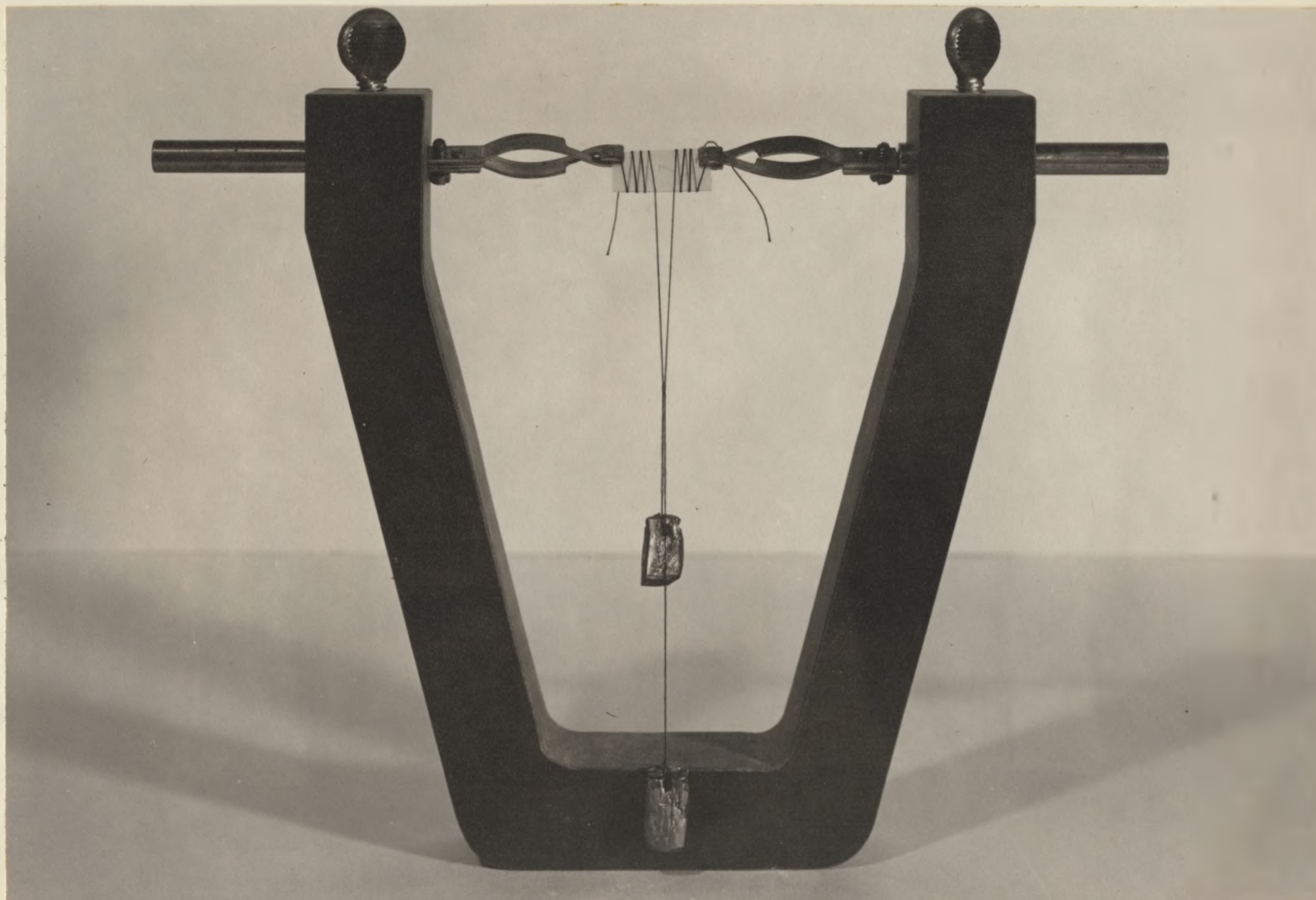

Figure 1. Jig Used in Winding Electrical Resistance Strain Elements

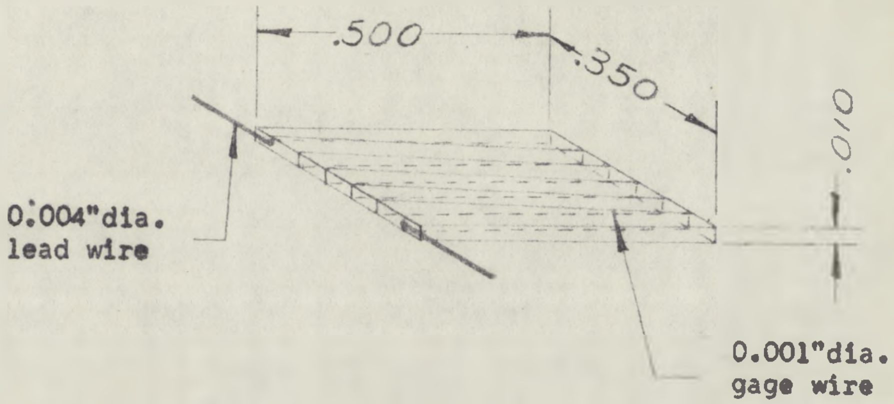

Figure 2. Electrical Resistance Strain Element

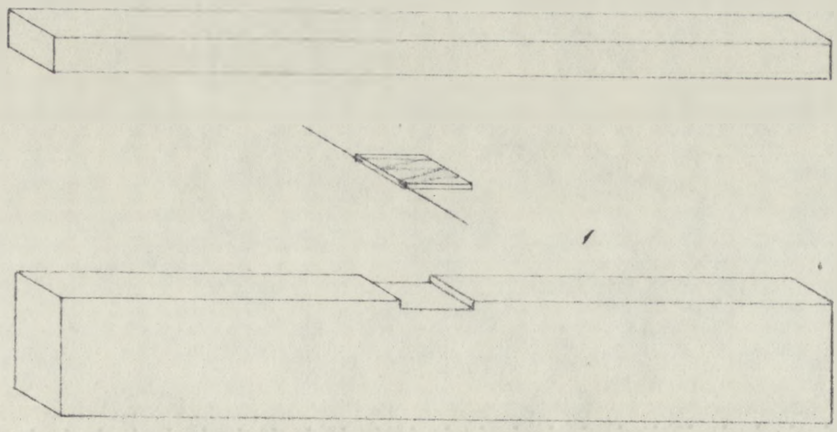

Figure 3. Method of Construction of Calibration Beam

cumine hydroperoxide was used successfully.

Castolite can be machined in several ways; by a high speed end mill or by turning on a lathe. Single point tools, high speeds, and light cuts result in the fewest machining stresses. The thin wafers used as gage backing were prepared by grinding on a 10" diameter no. 46 grit grinding wheel operating at 2400 RPM. The Cincinnati Milling Machine Company's "Cimcool" was used as a lubricant. Pieces were held in place during machining by either light mechanical pressure of by pressure sensitive tape.

Fourty-four gages were used in the construction of the model. Sixteen of these gages were constructed with a gage length of $\frac{1}{4}$". The remaining 28 had a gage length of $\frac{1}{2}$". The $\frac{1}{4}$" gages had a resistance of $119.9^{\pm .6}$ ohms. The $\frac{1}{2}$" gages had a resistance of $118.9^{\pm .6}$ ohms. The actual resistance of each gage is given in the appendix. These resistances were measured as shown in figure 4. The strain gage was connected in parallel with the 438 ohm resistor, which had been accurately calibrated, in order to obtain greater accuracy with the equipment available.

In order to determine the gage factor of the gages two samples of each type were imbedded in beam models as shown in figure 3. The milled slot in the beam should be approximately 0.003" deeper and 0.010" wider than the gage to allow for the lead wires. The entire assembly was then glued together and cured completely. The beam was then loaded as shown in figure 5. Strain readings were taken on a Baldwin portable strain indicator with the gage factor set at 2.0. A photograph of this set up is shown in figure 6. Deflection of the beam was measured by the dial indicator. The actual strain

cumine hydroperoxide was used successfully.

Castellite can be machined in several ways; by a high speed end mill, or by turning on a lathe. Single point tools, high speeds, and light cuts result in the fewest machining stresses. The thin wafers used as gage backing were prepared by grinding on a 10" diameter, 60 grit grinding wheel operating at 2400 RPM. The Cincinnati Milling Machine Company's "Cimcool" was used as a lubricant. Pieces were held in place during machining by either light mechanical pressure or by pressure sensitive tape.

Forty-four gages were used in the construction of the model. Fifteen of these gages were constructed with a gage length of ¼". The remaining had a gage length of ½". The ½" gages had a resistance of [illegible] ohms. The ¼" gages had a resistance of [illegible] ohms. The actual resistance of each gage is given in the appendix. These resistances were measured as shown in figure 4. The strain gage was connected in parallel with a 438 ohm resistor which had been accurately calibrated, in order to obtain greater accuracy with the equipment available.

In order to determine the gage factor of the gages two samples of each type were imbedded in beam models as shown in figure 5. The mid-span of the beam should be approximately 0.005" deep and 0.010" wider than the gage to allow for the lead wires. The entire assembly was then placed in an oven and cured completely. The beam was then loaded as shown in Figure 6. Strain readings were taken on a Baldwin portable strain indicator with the gage factor set at 2.0. A photograph of this set up is shown in Figure 7. Deflection of the beam was measured by the dial indicator. The beam's strain

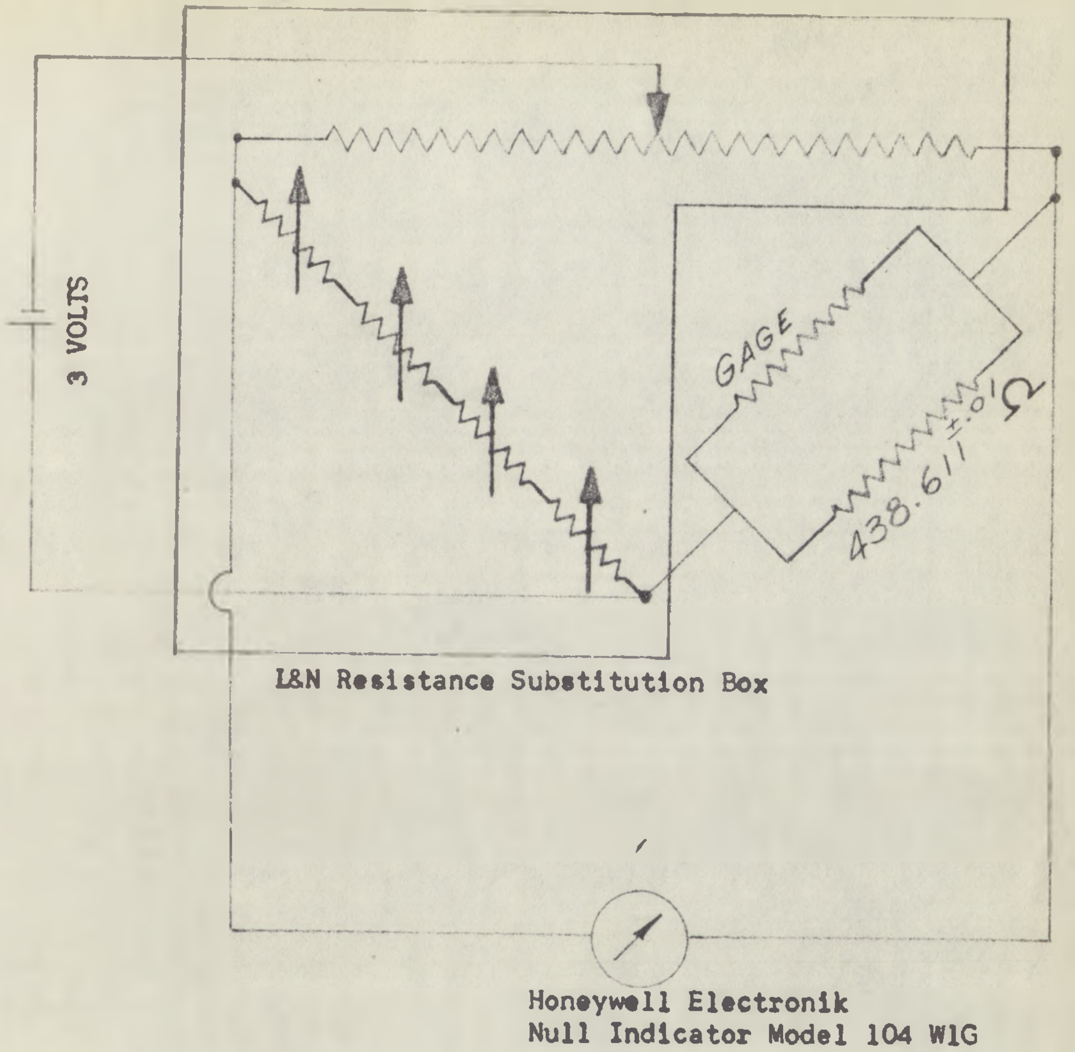

Figure 4. Schematic Circuit for Measuring Resistance of Strain Elements

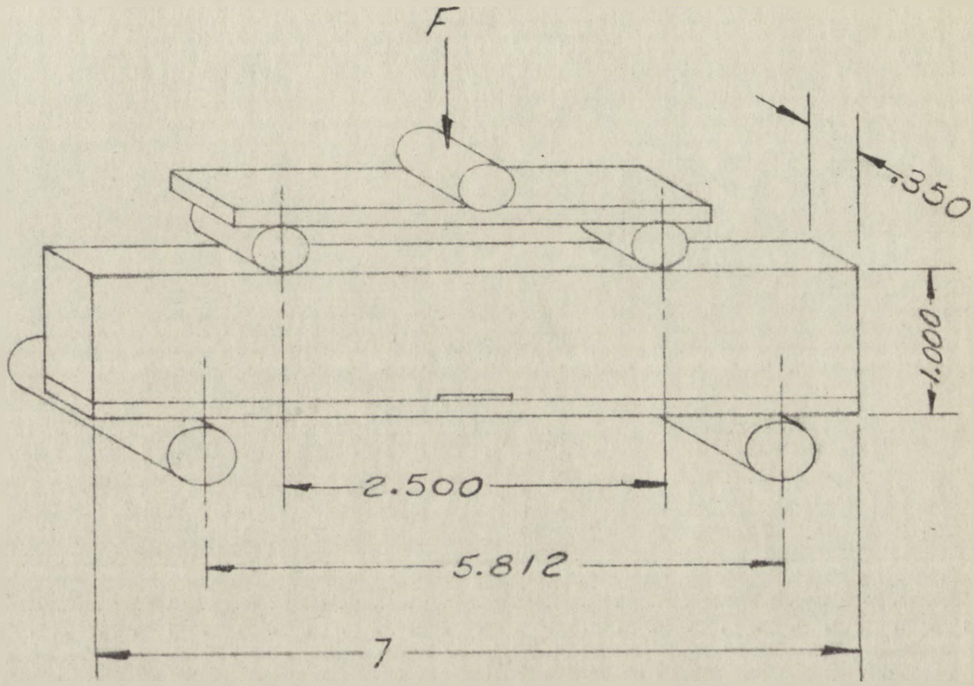

Figure 5. Dimensions and Method of Loading of Calibration Beam

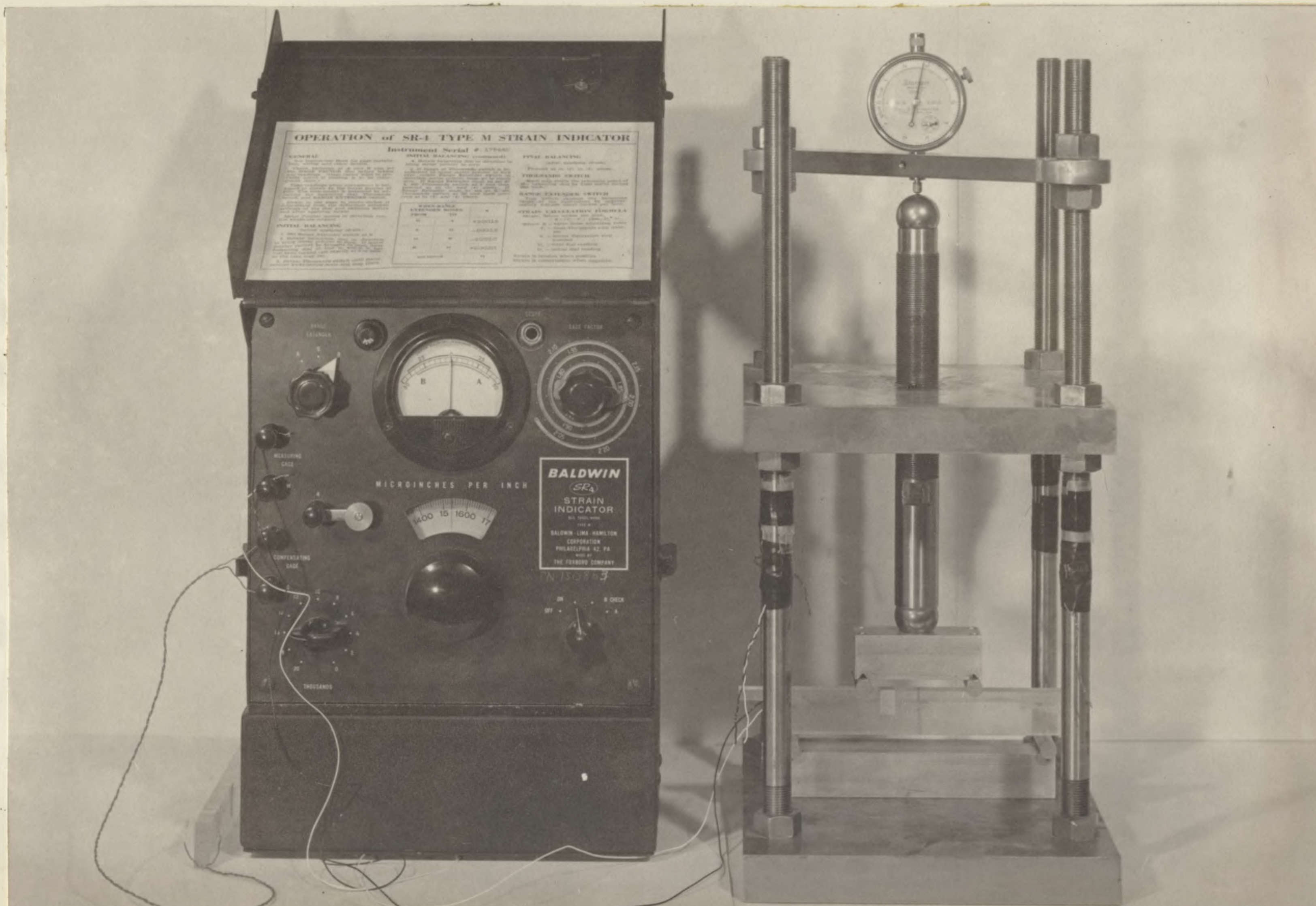

Figure 6. Experimental Determination of Gage Factor by Means of Calibration Beam

can be calculated from this measured deflection and the dimensions of the beam. Deflections of the loading apparatus were measured by means of SR-4 gages and found to introduce an error of less than 1% into the experiment. If significant, an allowance could be made for this deflection when calculating the actual gage factor.

The actual gage factor was then determined as follows:

For a beam, simply supported, two concentrated loads, the equation for the elastic deflection curve is:

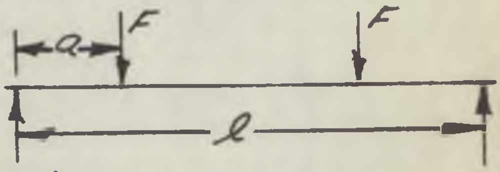

$$EI\frac{d^2y}{dx^2} = -M$$

Substituting the value of the bending moment:

$$EI\frac{d^2y}{dx^2} = -Fx \qquad x \leqq a$$

$$EI\frac{d^2y}{dx^2} = -Fa \qquad x \geqq a$$

Integrating these equations:

$$EI\frac{dy}{dx} = -\frac{Fx^2}{2} + C_1 \qquad x \leqq a \text{ --- } (1)$$

$$EI\frac{dy}{dx} = -Fax + C_2 \qquad x \geqq a \text{ --- } (2)$$

At X=a the slopes given by the two equations are equal, therefore, substituting X=a and equating equations 1&2:

$$-\frac{Fa^2}{2} + C_1 = -Fa^2 + C_2$$

$$C_1 = -\frac{Fa^2}{2} + C_2$$

Substituting this value into equations 1&2:

$$EI\frac{dy}{dx} = -\frac{Fx^2}{2} - \frac{Fa^2}{2} + C_2 \qquad x \leqq a \text{ --- } (3)$$

$$EI\frac{dy}{dx} = -Fax + C_2 \qquad x \geqq a \text{ --- } (4)$$

[illegible]

[illegible]

[illegible]

[illegible]

[illegible]

[illegible]

For a bend, [illegible]

[illegible]

[illegible]

[illegible]

[illegible]

[illegible]

[illegible]

[illegible]

[illegible]

At $x = \frac{l}{2}$, $\frac{dy}{dx} = 0$ So from equation 4:

$$0 = -Fa\frac{l}{2} + C_2 \qquad C_2 = Fa\frac{l}{2}$$

Replacing C_2 in equations 3&4 by this value:

$$EI\frac{dy}{dx} = -\frac{Fx^2}{2} - \frac{Fa^2}{2} + Fa\frac{l}{2} \qquad x \leqq a$$

$$EI\frac{dy}{dx} = -Fax + Fa\frac{l}{2} \qquad x \geqq a$$

Integrating again:

$$EIy = -\frac{Fx^3}{6} - \frac{Fa^2x}{2} + Fa\frac{l}{2} + C_3 \qquad x \leqq a \text{ -- (5)}$$

$$EIy = -\frac{Fax^2}{2} + Fax\frac{l}{2} + C_4 \qquad x \geqq a \text{ -- (6)}$$

At x=a the deflections given by equations 5&6 are equal, therefore by substituting x=a and equating equations 5&6:

$$-\frac{Fa^3}{6} - \frac{Fa^3}{2} + Fa^2\frac{l}{2} + C_3 = -\frac{Fa^3}{2} + Fa^2\frac{l}{2} + C_4$$

Which simplifies to:

$$-\frac{Fa^3}{6} + C_3 = C_4 \qquad \text{- - - - (7)}$$

At x=0, y=0 Then C_3=0 from equation 5 and $C_4 = -\frac{Fa^3}{6}$ from equation 7.

Substituting for C_3 and C_4 in equations 5&6 gives:

$$EIy = -\frac{Fx^3}{6} - \frac{Fa^2x}{2} + Fa\frac{l}{2}x \qquad x \leqq a \text{ --- (8)}$$

$$EIy = -\frac{Fax^2}{2} + Fax\frac{l}{2} - \frac{Fa^3}{6} \qquad x \geqq a \text{ --- (9)}$$

At x=a equation 8 or 9 gives:

$$EIy = -\frac{Fa^3}{6} - \frac{Fa^3}{2} + Fa^2\frac{l}{2}$$

From which:

$$y = \frac{Fa^2}{EI}\left[\frac{l}{2} - \frac{2a}{3}\right] \qquad \text{- - - (10)}$$

[illegible]

[illegible]

[illegible] is [illegible] [illegible]:

[illegible]

[illegible]

Integrating again:

[illegible]

[illegible]

[illegible] [illegible]

[illegible]

[illegible]

which simplifies to:

[illegible]

At [illegible] [illegible]

Substituting [illegible]

[illegible]

[illegible]

At the [illegible]

[illegible]

[illegible]

[illegible]

At the midpoint of the beam:

$$S = \frac{Mc}{I} = \frac{Fac}{I} = E\epsilon \qquad \frac{Fa}{EI} = \frac{\epsilon}{c}$$

Then equation 10 gives:

$$y = \frac{\epsilon a}{c}\left[\frac{l}{2} - \frac{2a}{3}\right] \quad --- \quad (11)$$

From the dimensions of the beam and the location of the gage $C = .240''$,

$\frac{l}{2} = 2.90625''$, $a = 1.65625''$ Rearranging equation 11 and substituting for C, a, & L:

$$\epsilon = \frac{Cy}{a\left[\frac{l}{2} - \frac{2a}{3}\right]} = \frac{.240 \times .005}{1.656\left[2.906 - \frac{2}{3}(1.656)\right]} \quad -- (11a)$$

From which:

$$\epsilon = .000402 \text{ IN./IN.}$$

For the calibration test:

$$\text{G.F.}_{(\text{assumed})} = 2 = \frac{\frac{\Delta R}{R}}{\epsilon\,(\text{READ})} \quad --- \quad (12)$$

But since the strain is known from equation 11a

$$\frac{\Delta R}{R} = \text{G.F.}\,(\text{ACTUAL})\ \epsilon_{(\text{CALCULATED})}$$

Substituting into equation 12:

$$2\epsilon_{(\text{READ})} = \text{G.F.}_{(\text{ACTUAL})}\ \epsilon_{(\text{CALCULATED})} = \text{G.F.}_{(\text{ACTUAL})} \times .000402$$

Therefore:

$$\frac{2\ \epsilon(\text{READ})}{.000402} = \text{G.F.}\,(\text{ACTUAL})$$

The actual measurements taken from each calibration beam are listed in the appendix. The calculated gage factors are shown in table 1.

The actual [illegible]

the appendix. [illegible]

Table 1. Gage factors determined from calibration beams

Gage Number	48	34	45	53
Gage Length	$\frac{1}{4}$"	$\frac{1}{4}$"	$\frac{1}{2}$"	$\frac{1}{2}$"
Gage Factor (Compression)	1.41	1.42	1.46	1.43
Gage Factor (Tension)	1.50	1.43	1.45	1.41

Gage factors were determined with the beams loaded both in tension and compression. As can be seen, little difference was found between the two cases.

The gage factors determined in the manner just outlined are valid only for this one model material and for a uniaxial stress field. To determine a gage factor suitable for a biaxial stress field it was necessary to measure the cross sensitivity of the gages. This was done by loading these same calibration gages transversly in direct compression and recording their output. The rosette gage factor could then be determined as follows:

From compression test S = 95 psi

From compression deflection test of Castolite specimens E was found to be 652,000 psi.

Poissons ratio for Castolite was found to be .39. This value was obtained by measuring the velocity of sound thru Castolite and making use of the known relationship between E, v, ν, & ρ. This calculation is included in the appendix.

$$\epsilon_t = \frac{S}{E} = \frac{95}{652,000} = .0001457 \text{ IN./IN.}$$ Compression

Table 1. Gage factors determined [illegible]

Gage Number	[illegible]	[illegible]	[illegible]	[illegible]
Gage Length	[illegible]	[illegible]	[illegible]	[illegible]
Gage Factor (Compression)	[illegible]	[illegible]	[illegible]	[illegible]
Gage Factor (Tension)	[illegible]	[illegible]	[illegible]	[illegible]

Gage factors were [illegible] compression, [illegible] gages.

The gage factors [illegible] for this one model [illegible] gage factor [illegible] the cross [illegible] calibration gages [illegible] output. The [illegible] gage factor [illegible]

From compression [illegible]

From compression [illegible]

[illegible]

[illegible]

[illegible]

[illegible]

in the [illegible]

ϵ_t (READ) = .000052 IN/IN. Tension

By the definition of gage factor:

$$G.F. = \frac{\frac{\Delta R}{R}}{\epsilon} \qquad \text{therefore: } \frac{\Delta R}{R} = 2 \times .000052 = -.0001457 \times G.F.$$

and $$G.F. = \frac{.000104}{-.0001457} = -.714$$

But: $$G.F._u = G.F._l \epsilon_l + G.F._t \epsilon_t \quad \text{- - - -} \quad (13)$$

For a uniaxial stress field:

$$\epsilon_t = -\nu \epsilon_l$$

Substituting into equation 13:

$$G.F._u \epsilon_l = G.F._l \epsilon_l - G.F._t \nu \epsilon_l$$

Dividing by ϵ_l

$$G.F._u = G.F._l - \nu G.F._t \quad \text{- - -} \quad (14)$$

Two values are known which can be substituted into equation 14. One was obtained from the flexure test where $GF_u = 1.45$. The second was obtained from the cross sensitivity test where $GF_u = -.714$. Substituting these values into equation 14 and solving the resulting two equations simultaneously for GF_l and GF_t gives:

$$-.714 = G.F._t - .39 G.F._l \quad \text{OR} \quad 1 = -1.401 G.F._t + .547 G.F._l$$

$$1.45 = G.F._l - .39 G.F._t \quad \text{OR} \quad 1 = .69 G.F._l - .269 G.F._t$$

$$.69 G.F._l - .547 G.F._l = -1.401 G.F._t + .269 G.F._t$$

$$.143 G.F._l = -1.132 G.F._t$$

$$G.F._l = -7.92 G.F._t$$

$$1.45 = -7.92\,G.F._t - .39\,G.F._t$$

$$G.F._t = -.175$$

$$G.F._\ell = (-7.92)(-.175) = 1.38$$

From the definition of cross sensitivity:

$$k = \frac{G.F._t}{G.F._\ell} = \frac{-.175}{1.38} = -.127 = -12.7\,\%$$

The rosette gage factor GF_r is then determined as:

$$G.F._R = \frac{G.F._u\,(1-k^2)}{1-\nu k} = \frac{1.45[1-(-.127)^2]}{1-(.39)(-.127)}$$

$$G.F._R = \frac{1.45(1-.016)}{1+.049} = 1.360$$

The actual measurements taken in the cross sensitivity tests are listed in the appendix.

V. DETERMINATION OF THE STRESS DISTRIBUTION IN A PLASTIC MODEL NEAR AN ELECTRICAL RESISTANCE STRAIN ELEMENT

The inclusion of a strain element in a plastic model introduces the possibility that the gage wire will reinforce the plastic. While the wire has a very small cross section, it does possess a much higher modulus than the model material and any reinforcing effect would alter the stress pattern within the model. Therefore, an investigation into the stress state around an imbedded gage was undertaken by means of a photoelastic analysis. For this purpose, sample beams of the model material were made up, polished, and examined in a photoelastic polariscope. Light field photoelasticity (polarizer and analizer parallel, quarter wave plates crossed) was used in every case. All beams had dimensions of 0.350" x 1.000" x 7.0". Figure 7 shows a plain Castolite beam loaded at two points and simply supported at the ends. The area between the two load points is subjected to a constant bending moment and the dark (fringe) lines are lines of constant shearing stress. Figure 8 shows a similar beam with a strain element imbedded in it. The gage is oriented lengthwise along the beam. The outline of its edge can be seen in the lower center portion of the beam. The significant feature of this photograph is that although a fringe line runs through the gage a comparison with figure 7 shows no change in the fringe pattern. Figure 9 shows the same beam as figure 8 but with additional load applied to shift the fringe pattern so that the gage is now between two fringe lines. Once again there is no change in the stress distribution. Figure 10 shows a beam with a gage oriented vertically at its center. Here a slight but insignificant disturbance can

V. DETERMINATION OF THE STRESS DISTRIBUTION IN A PLASTIC MODEL NEAR AN ELECTRICAL RESISTANCE STRAIN ELEMENT

The inclusion of a strain element in a plastic model introduces the possibility that the gage wire will reinforce the plastic. While the wire has a very small cross section, it does possess a much higher modulus than the model material and any reinforcing effect would alter the stress pattern within the model. Therefore, an investigation into the stress state around an embedded gage was undertaken by means of a photoelastic analysis. For this purpose, sample beams of the model material were made up, polished, and examined in a photoelastic polariscope. Light field photoelasticity (polarizer and analyzer parallel, quarter wave plates crossed) was used in every case. All beams had dimensions of 0.250" x 1.000" x 7.0". Figure 7 shows a plain Castolite beam loaded at two points and simply supported at the ends. The area between the two load points is subjected to a constant bending moment and the dark (fringe) lines are lines of constant shearing stress. Figure 8 shows a similar beam with a strain element imbedded in it. The gage is oriented lengthwise along the beam. The outline of its edge can be seen in the lower center portion of the beam. The significant feature of this photograph is that although a fringe line runs through the gage a comparison with Figure 7 shows no change in the fringe pattern. Figure 9 shows the same beam as Figure 8 but with additional load applied to shift the fringe pattern so that the gage is now between two fringe lines. Once again there is no change in the stress distribution. Figure 10 shows a beam with a gage oriented perpendicularly at its center. Here a slight but insignificant disturbance can

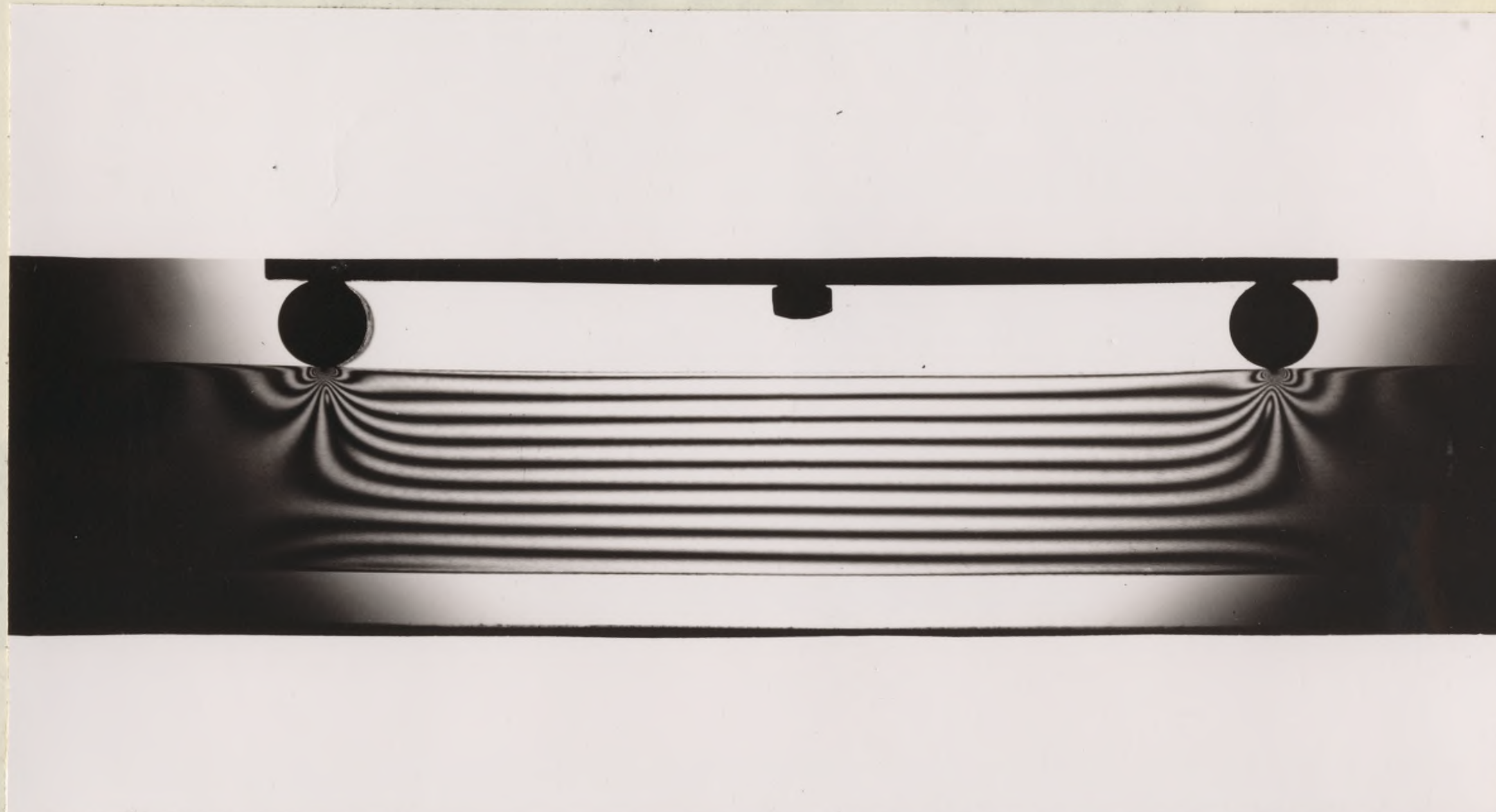

Figure 7. Plain Castolite Photoelastic Model

Load = 176.9 lbs.

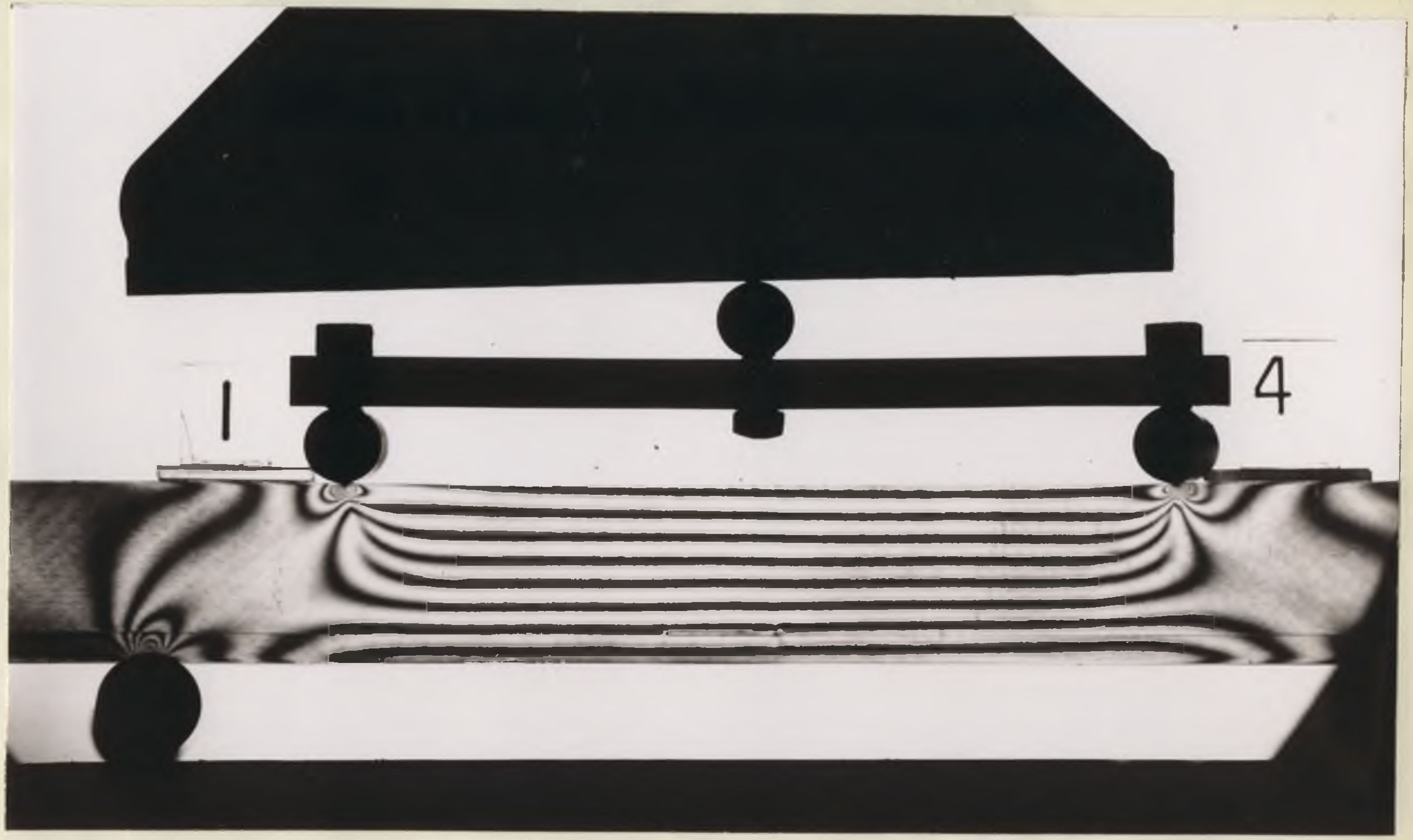

Figure 8. Strain Element Imbedded in Photoelastic Model

Plane of Gage Parallel to Edge of Beam

Load = 176.9 lbs.

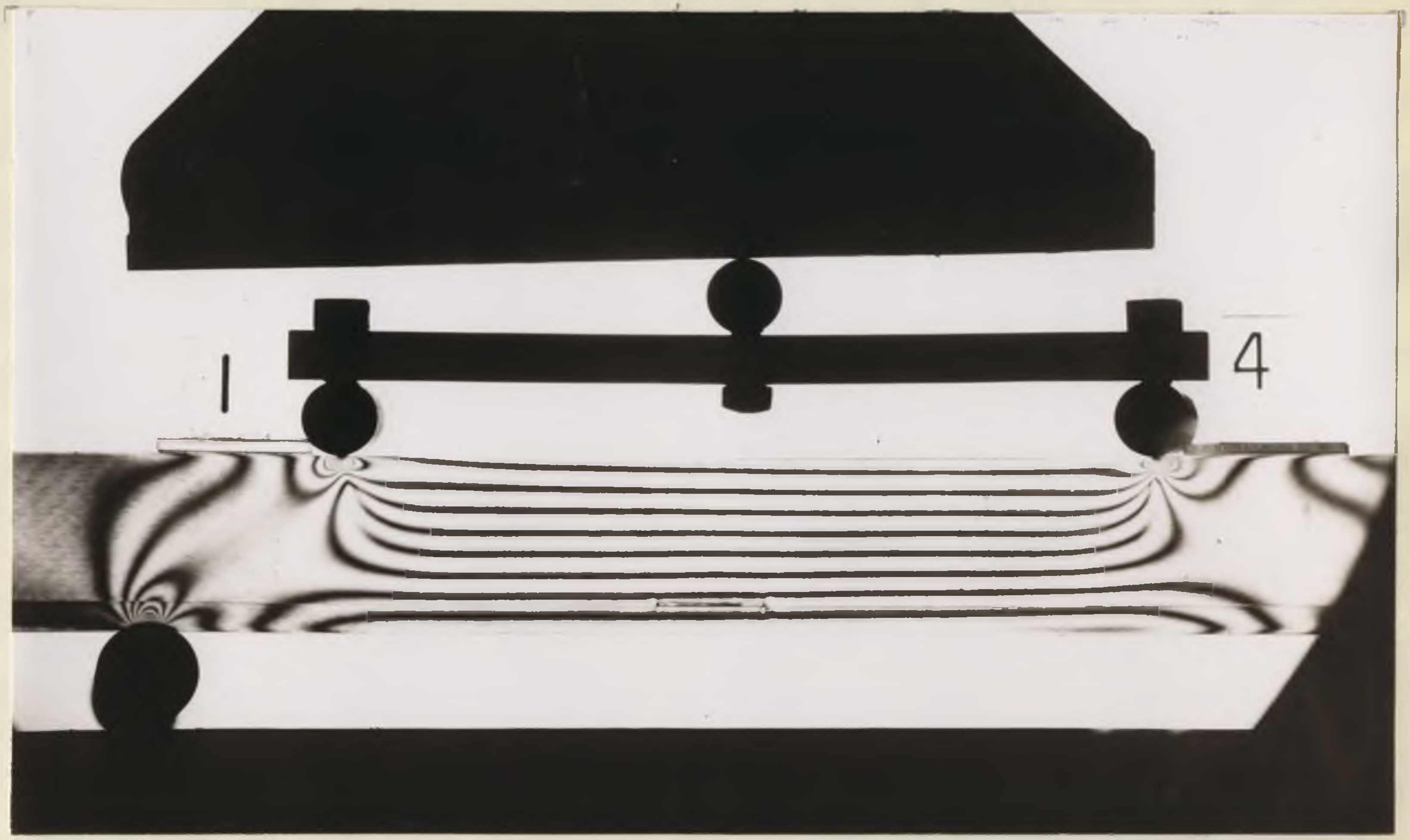

Figure 9. Strain Element Imbedded in Photoelastic Model

Plane of Gage Parallel to Edge of Beam

Load = 191.3 lbs.

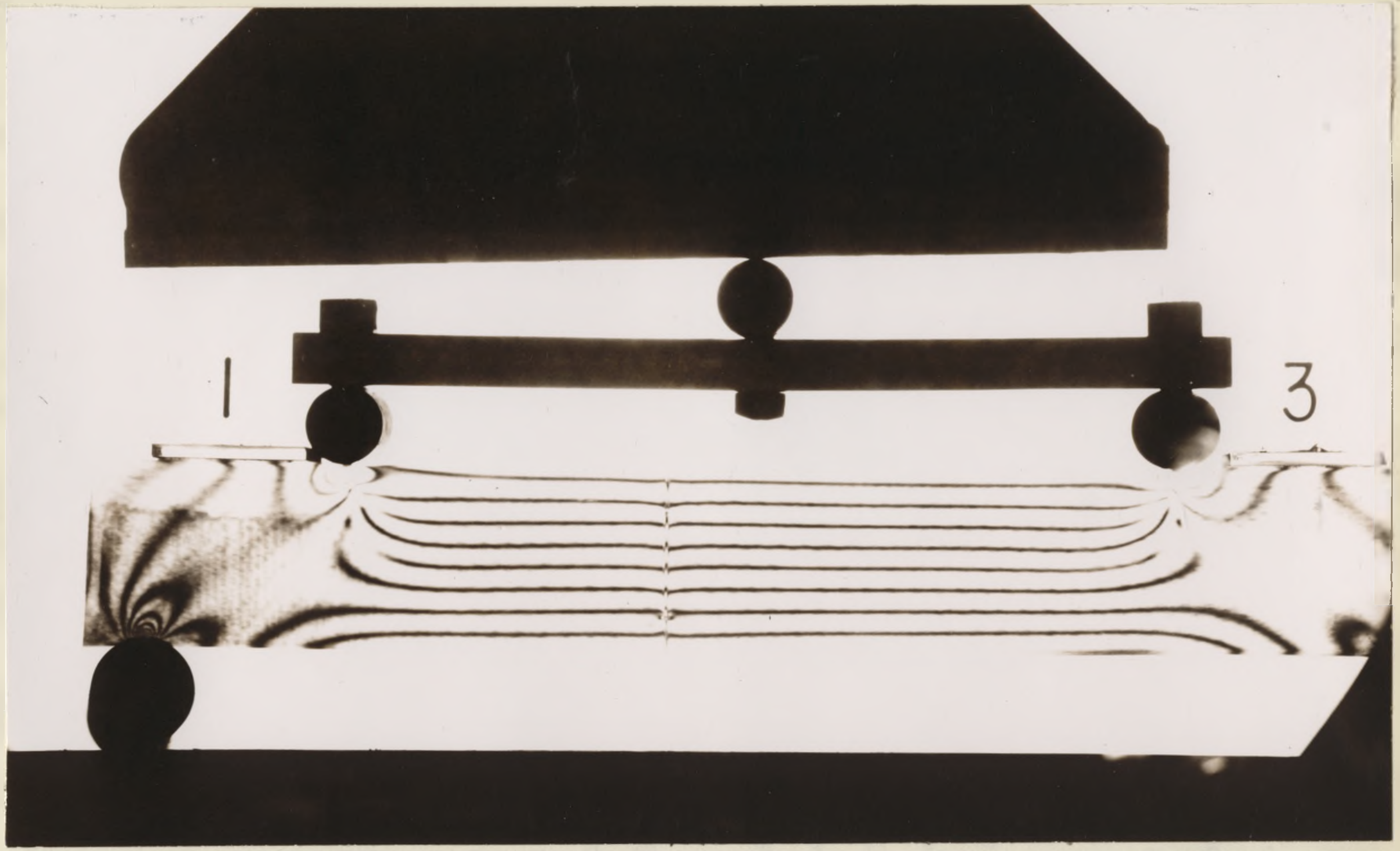

Figure 10. Strain Element Imbedded in Photoelastic Model

Plane of Gage Parallel to End of Beam

Load = 176.9 lbs.

be noted at the vertical surfaces of the gage. The ripple effect which can be seen in this photograph is due to a grinding operation on the face of the beam. This could have been eliminated by additional polishing of the surface. In figure 11 the gage element is in a plane parallel to the plane of the picture. If the resolution of the photograph were sufficiently great the grid pattern of the 0.001" diameter wire could be seen. The small circles in the gage area are air pockets trapped when the gage was cemented in place. No disturbance in the fringe pattern is noted here. Figure 12 shows a beam containing approximately 5 inches of 0.004" diameter lead wire. Here the disturbance of the fringe pattern is more noticeable. However, since this would occur not in the center of the gage but leading away from one edge it is not considered serious.

It was found that Castolite will exhibit stresses along a machined surface if care is not taken in machining, and even if unstressed initially, it will develop stresses with time. Figures 8 through 12 all show time edge stresses. Machining stresses can be relieved by annealing at a temperature of 200°F and cooling slowly. It was found that the material was less susceptable to machining stresses if annealed prior to machining. Figure 13 shows a drilled specimen after annealing.

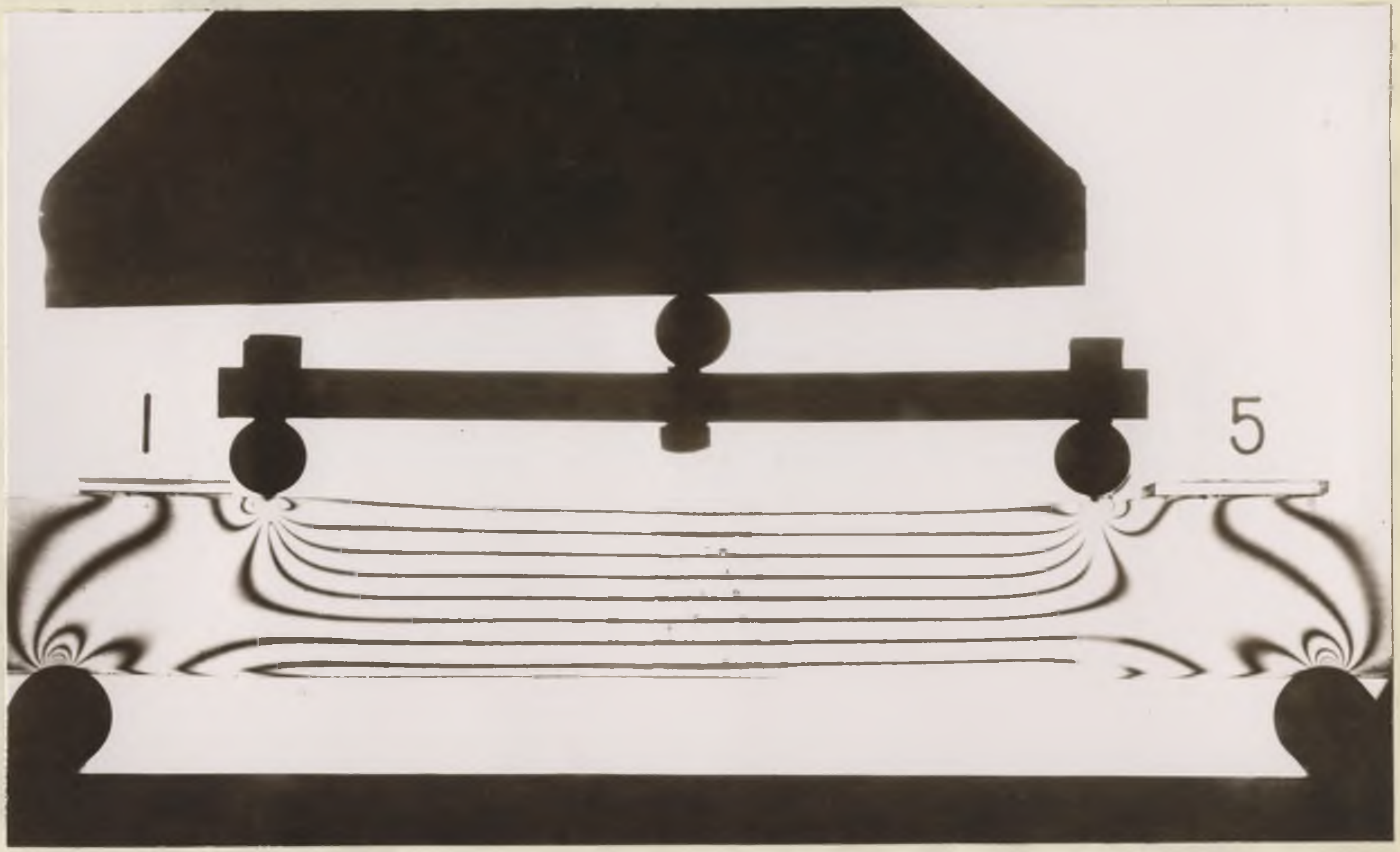

Figure 11. Strain Element Imbedded in Photoelastic Model

Plane of Gage Parallel to Face of Beam

Load = 176.9 lbs.

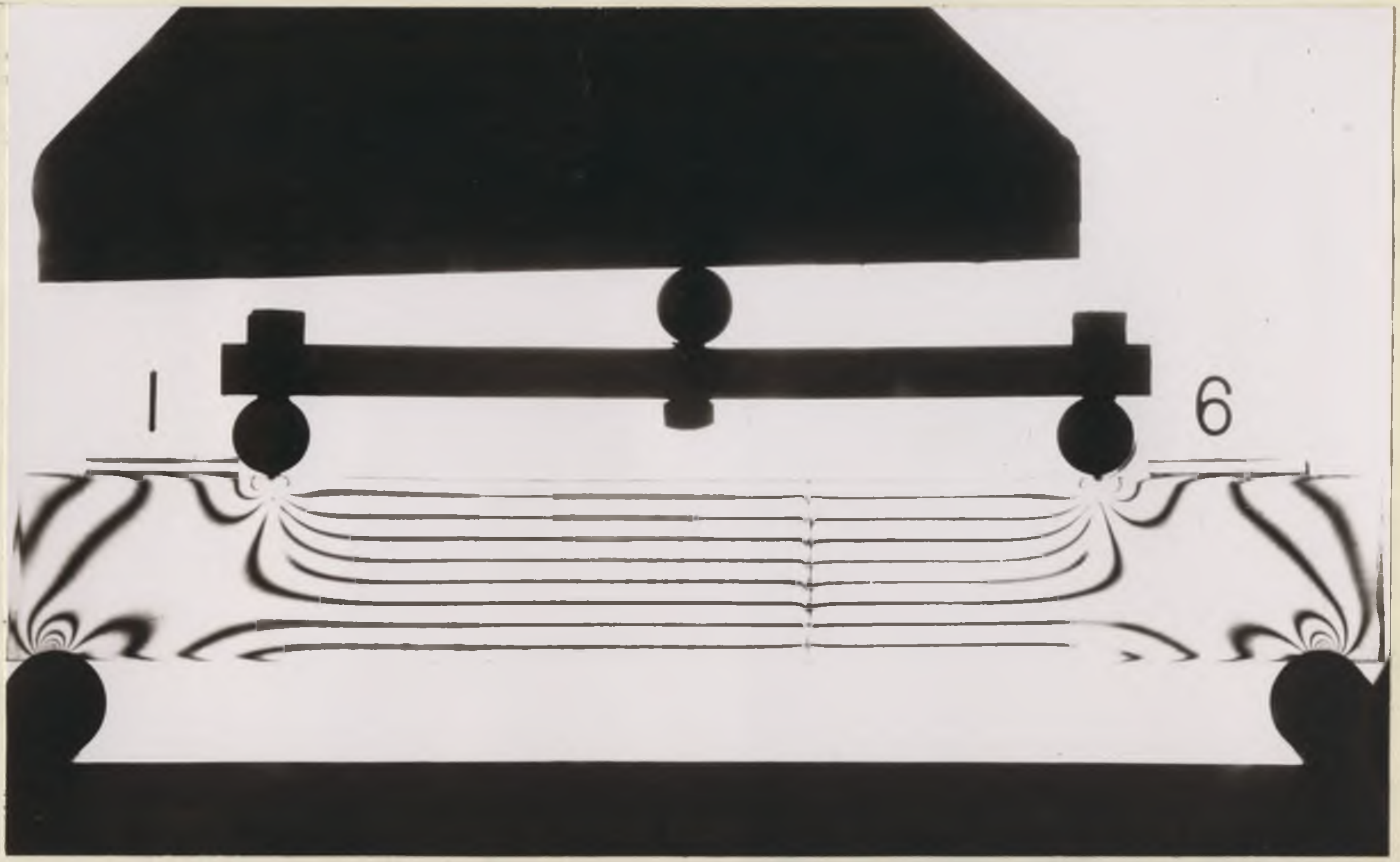

Figure 12. 0.004 Inch Diameter Lead Wire Imbedded in Photoelastic Model

Plane of Wire Parallel to End of Beam

Load = 176.9 lbs.

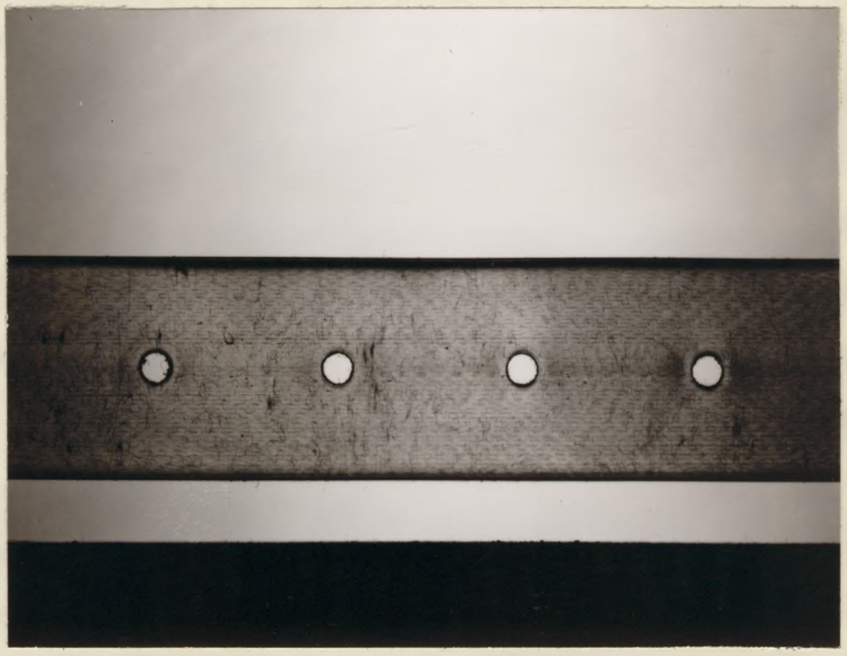

Figure 13. Holes Drilled in Castolite Specimen

VI. EXPERIMENTAL INVESTIGATION

The purpose of the experimental investigation was to find the stress distribution at internal points of a thick wall pressure vessel, and in particular, the stress concentration factor K_t at the fillets of the upper and lower flanges. The effect of varying the fillet radius was also investigated.

Prior to testing the pressure vessel model, gages of each type were imbedded in beams of the model material and subjected to calibration tests. This also gave a measure of the accuracy and reproducability of the experiment.

The completed model contained 44 strain gages located as shown in figures 14 and 15. Gages 1 through 12 were located at the inner diameter, center of wall, and outer diameter of the straight cylindrical section. There were four sets of these gages. Two sets were oriented in a longitudinal direction and two sets were oriented in a circumferential direction. The stresses at these points could be calculated by thick wall vessel formulae. A comparison of calculated and measured values here gave an additional check on the accuracy of the experiment.

Due to a series of mishaps no more than thirty gages were active at any one time. However, three complete rosettes were always active in the center section of the model so that comparison with theory could be made.

In the experiment, internal pressure was applied to the vessel in increments and the gage readings taken at each step. Three such tests were run. One with an upper fillet radius of 3/4", one with an upper fillet radius of 1/2", and one with an upper fillet radius of 1/4". As an additional test

[illegible]

The purpose of the [illegible]

distribution [illegible]

particular, the [illegible]

and lower [illegible]

gated.

Prior to [illegible]

imbedded in [illegible]

This also [illegible]

The complete [illegible]

14 and [illegible]

well, and [illegible]

four sets of [illegible]

and two sets [illegible]

these points [illegible]

of calculation and [illegible]

accuracy of the [illegible]

Due to a [illegible]

one time, however, [illegible]

section of the [illegible]

In the [illegible]

increments [illegible]

run. One [illegible]

of 1/2", [illegible]

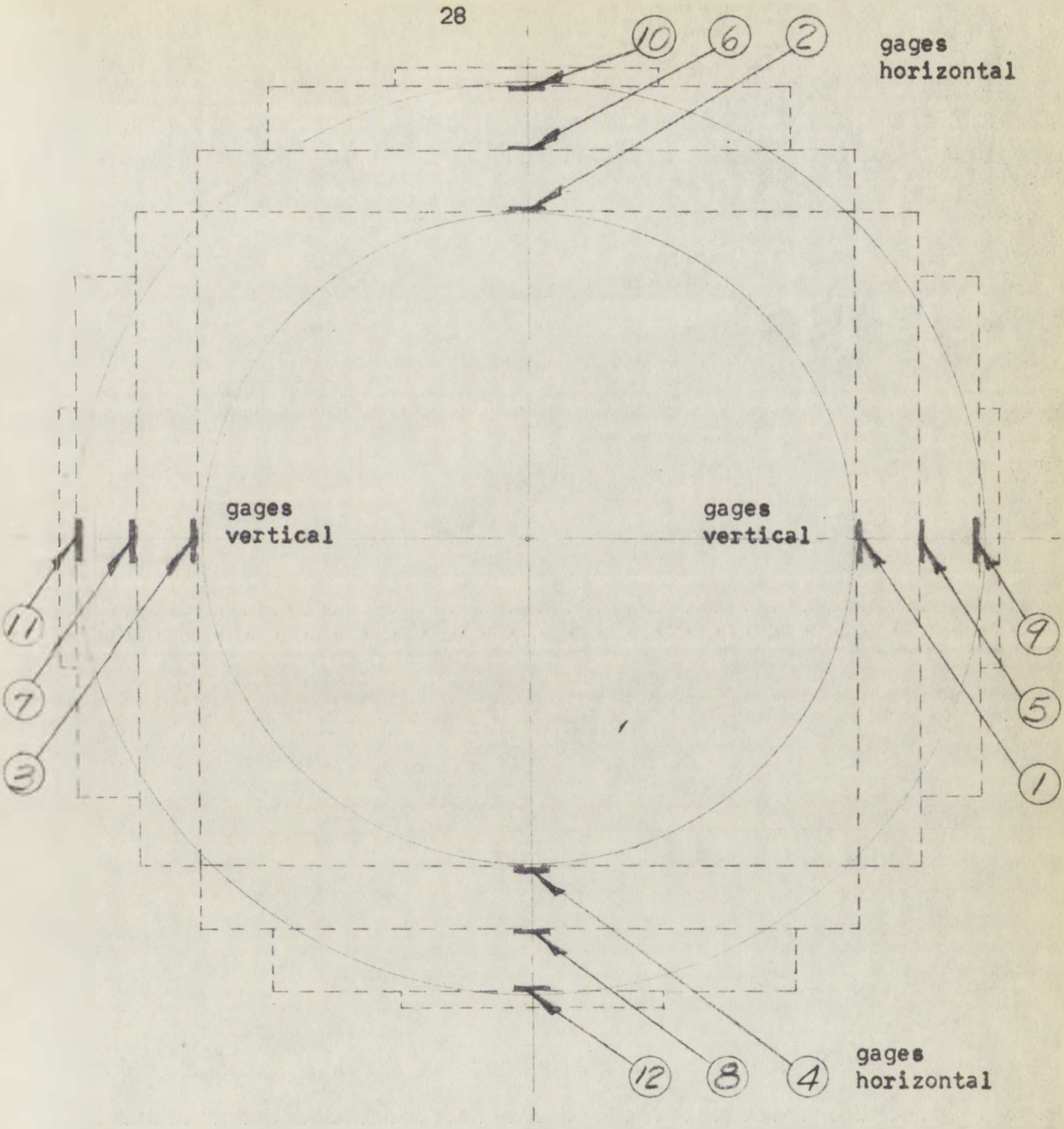

Figure 14. Section Showing Method of Construction and Location of Gages

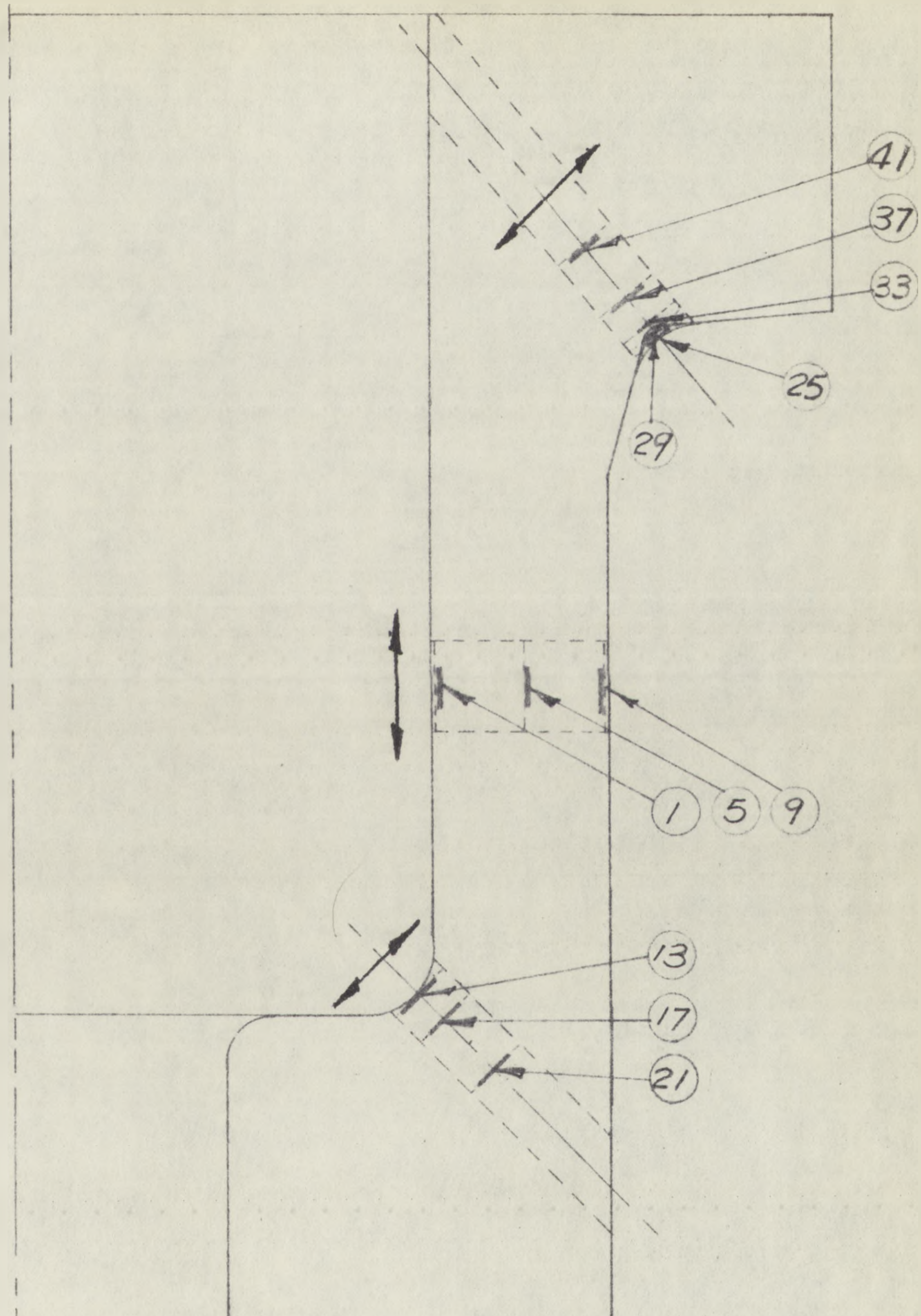

Figure 15. Section showing Method of Construction and Location of Gages

The gage orientation is indicated by arrows.

a series of loads was applied to the pull bar on the bottom plate of the model. This was done since the loading on the prototype is a combination of these two loadings.

Experimental data were compared with calculated values whenever possible.

VII. THEORETICAL INVESTIGATION

The stresses in a uniform straight cylindrical section of a vessel subjected to internal pressure can be obtained from the geometry of the vessel and the applied forces. Murphy (9)* gives these relationships:

$$S_t = \frac{P_i r_i^2 - P_o r_o^2 + \frac{r_i^2 r_o^2}{r^2}(P_i - P_o)}{r_o^2 - r_i^2}$$

and:

$$S_\ell = \frac{r_i^2 P_i}{(r_o - r_i)^2}$$

For the model in question, $r_i = 5"$ $r_o = 7"$. r, the coordinate of the stress, = 5.032" at the inner gage location. Then:

$$S_t \Big|_{r=5.032} = 3.057\, P_i \quad \text{PSI}$$

$$S_\ell = 1.04\, P_i \quad \text{PSI}$$

At discontinuities in the section, it is customary to apply a stress concentration factor as an allowance for the change in geometry. Peterson (10) gives a listing of factors for various geometries and loading conditions. The case selected as being most nearly applicable to the problem at hand was that of a T-head with a distributed load. A section through the cylindrical wall of the vessel, where it joins the flange, resembles one-half of a standard T-head.

At the lower flange of the vessel the correct factor for a 3/4" radius (r/d = .187) would appear to be approximately 3.5. This would make the maximum stress at that point = 10.7 P_i psi.

---

* Numerals in parenthesis refer to corresponding items under the heading, " LITERATURE CITED ".

At the upper flange of the vessel the correct factor for a 3/4" radius (r/d = .187) is 3.5, for a 1/2" radius (r/d = .125) 4.5, and for a 1/4" radius (r/d = .062) 6.5. This would make the maximum stresses = 10.7 P_1, 13.8 P_1, and 19.9 P_1 psi respectively.

VIII. APPARATUS

A cross section of the model is shown in figure 16. This model is a 1/4 scale, Castolite plastic, model of the outer jacket of a thick wall pressure vessel. The model was constructed of sheets of plastic cemented together. The laminations were approximately 1" in thickness. Larger castings could not be poured because of the undesirable exotherm which leads to highly stressed castings.

Two techniques were used to imbed the gages in the model. One method was to make up sections of the vessel from strips of Castolite which had the gage elements cemented between them. This method was used to construct the calibration beams and was used on the center section of the model. Figure 14 shows how 12 gages were fitted between strips of plastic which made up the center section of the model. Figure 17 is a photograph of this array before it was cemented together. In the second method the model section was made up with no gages in it. Then a hole was drilled through the model and a plug containing the gages cemented in place. This method was used at the upper and lower fillets. Figure 15 shows how these plugs were located. It is a section through one of four identical locations. Figure 18 shows a photograph of one plug before it was assembled with the gages. Two sizes of gages were used. They had 1/2" and 1/4" gage lengths. The 1/4" gages were used in locations where a high stress gradient was expected; the 1/2" gages where a lower gradient was expected. It should be noted that even with the smaller gages the output represents the average strain in a volume 1/4" x 3/8" x .012". The 0.004" diameter lead wires were brought out through the

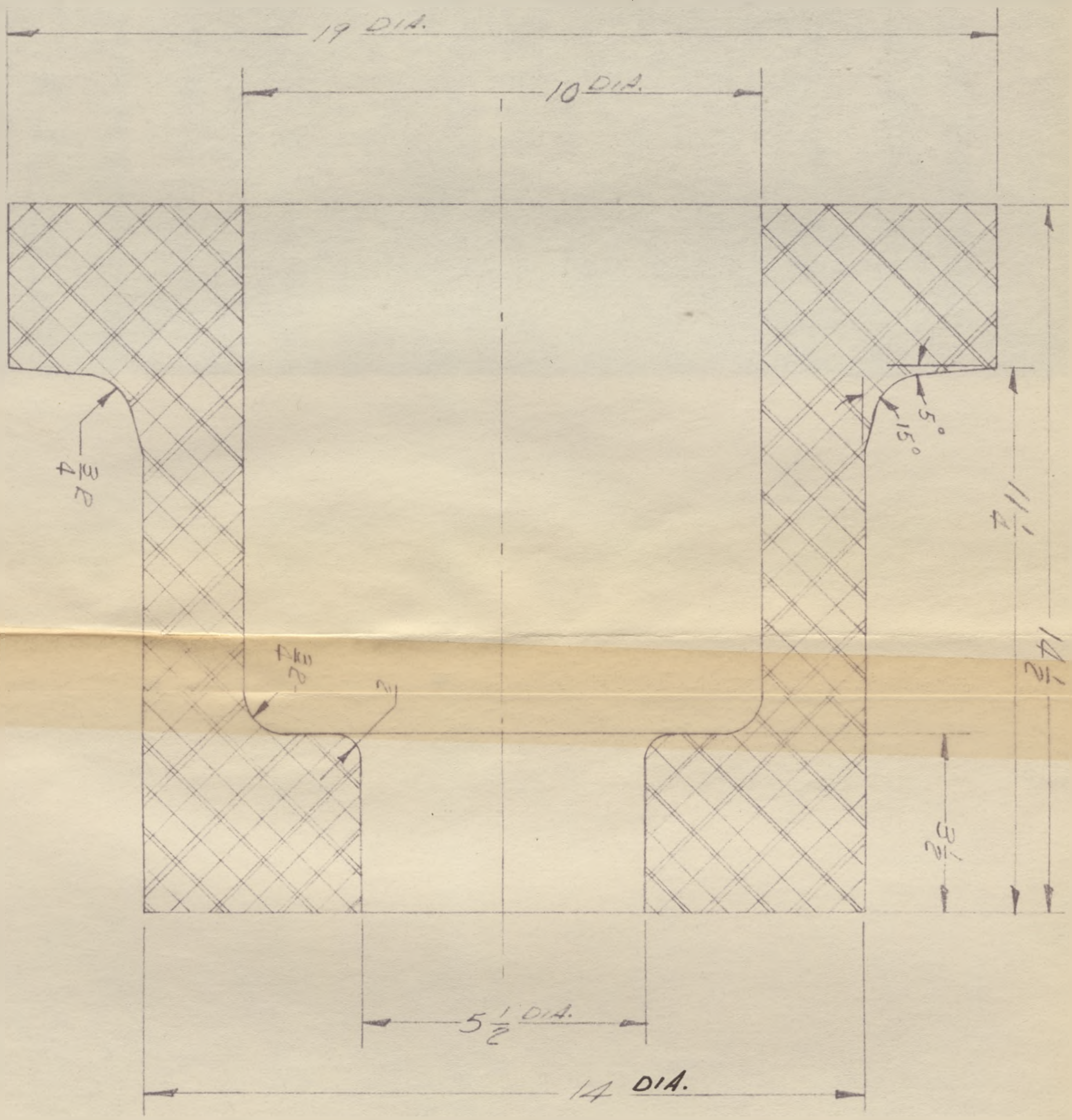

Figure 16. Cross Section of Pressure Vessel Model

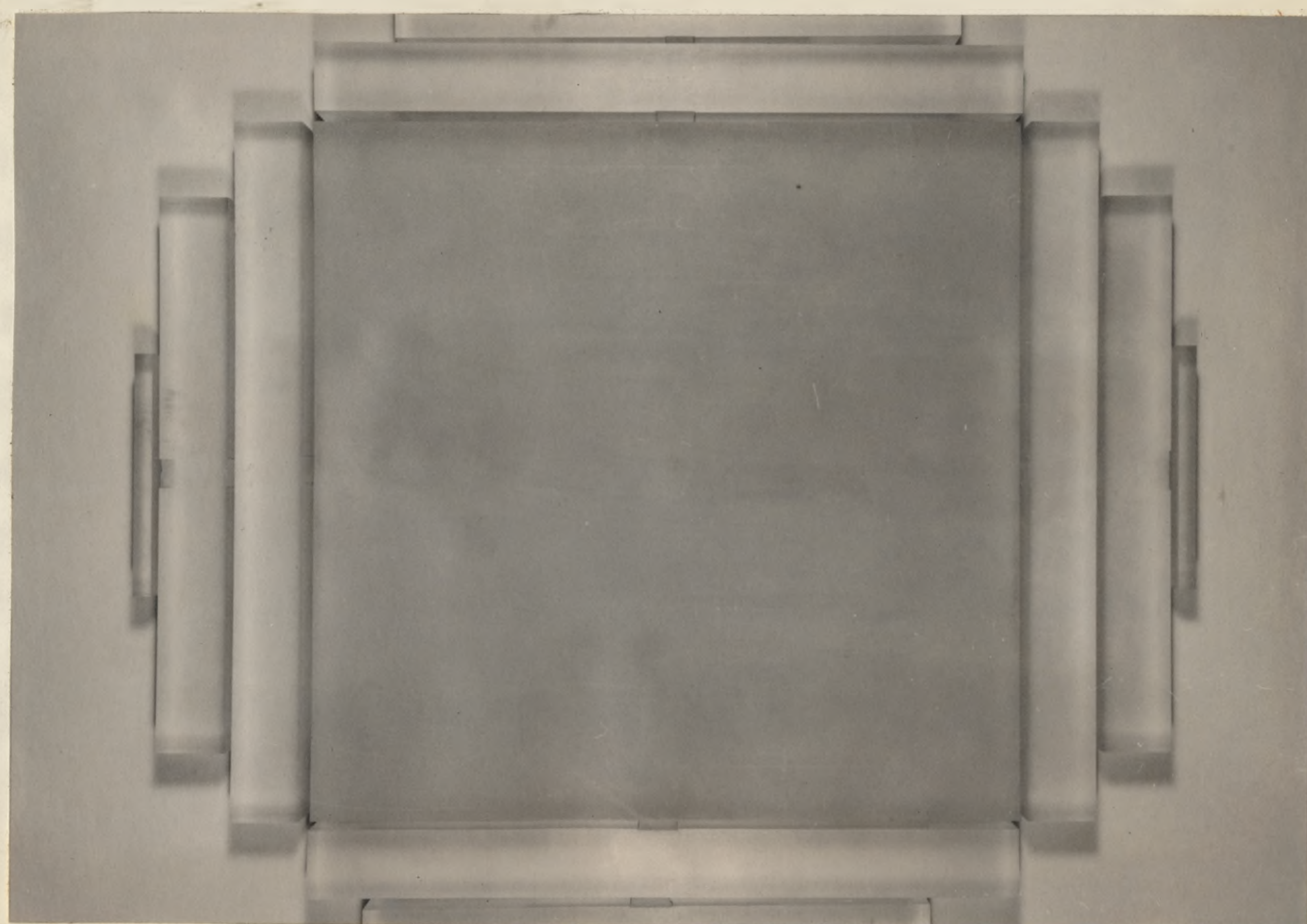

Figure 17. Center Section of Pressure Vessel Before Assembly

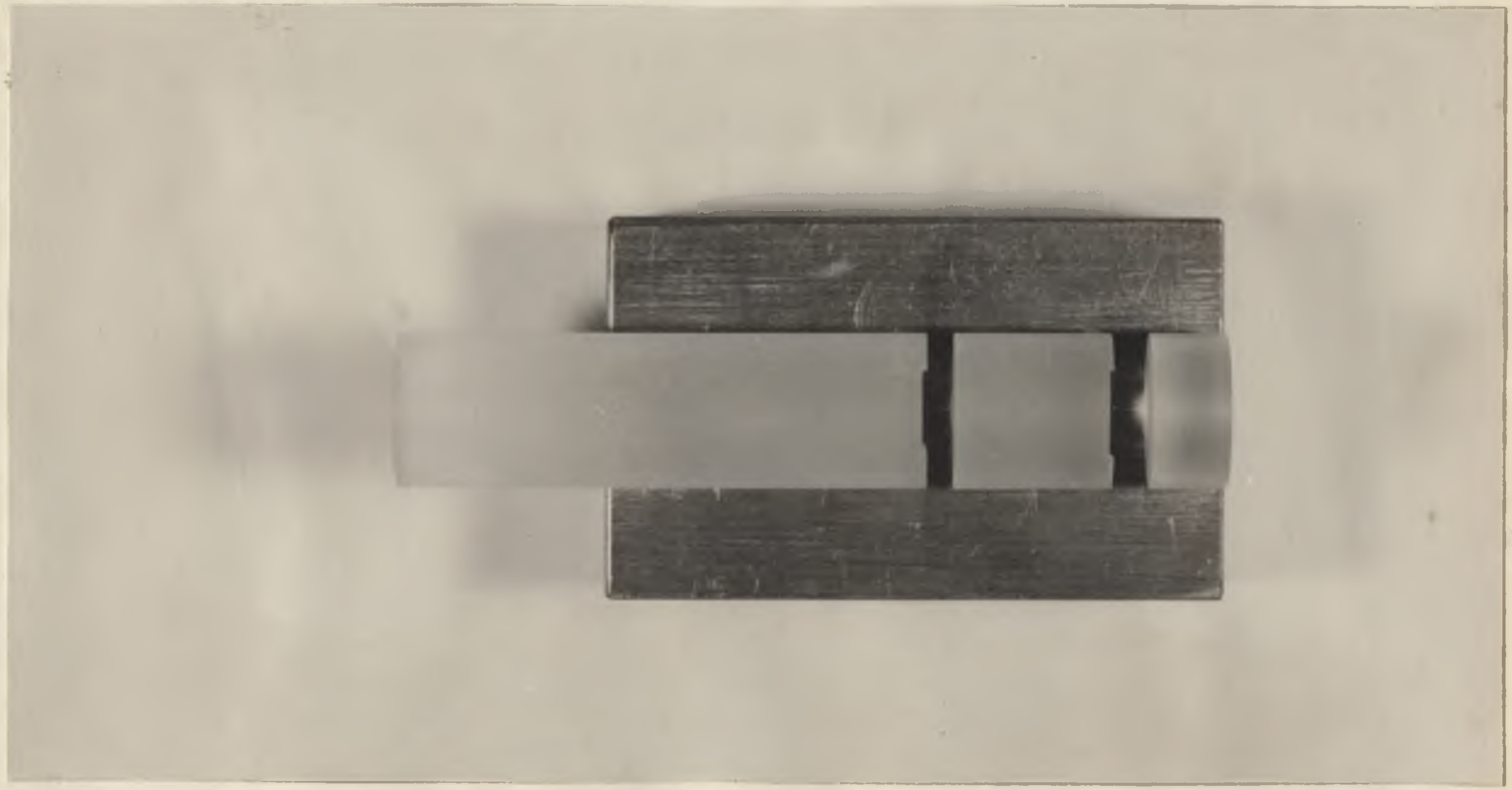

Figure 18. Castolite Plug Before Assembly

wall of the model and connected to larger wires which run to the strain indicator. Figure 19 is a photograph of some of these wires where they emerge from the model. Figure 20 is a photograph showing the interior of the model with the gage leads as they are brought out of the top.

Figure 21 is a cross sectional sketch of the test assembly. At first, hydraulic fluid was contained in a rubber bag the mouth of which served as a gasket between the top plate and the top flange of the pressure vessel. However, this set-up invariably leaked so an automobile inner tube was used with the valve protruding through a hole in the top plate. Figure 22 is a photograph of this test set-up. Figure 23 is a closer view showing the model suspended in the holding fixture.

During the loading test it was found that it was impractical to attach the needed weights to the pull bar. Therefore, the bar was reversed and brought out through a hole in the top plate and the entire assembly loaded in a hydraulic press. A photograph of this set-up is shown in figure 24.

A Baldwin portable strain indicator was used for all strain readings.

[illegible] of the model was [illegible] [illegible] [illegible]

[illegible]. Figure 20 is a [illegible] of one of these [illegible]

[illegible] from the model. Figure 21 is a [illegible]

the model [illegible]

Figure 22 is a cross sectional [illegible]

[illegible] was [illegible] in a [illegible] and the depth of which [illegible]

[illegible] the plate and the [illegible] of the pressure [illegible]

[illegible]

[illegible] in the top plate. Figure 23 is a

[illegible]. Figure 24 is a closer view [illegible]

[illegible]

During the testing [illegible]

[illegible]

[illegible] through a hole in the top plate and the [illegible]

[illegible] a photograph of this [illegible]

[illegible]

Figure 19. Outer Surface of Model Showing Lead Wires Emerging From Interior

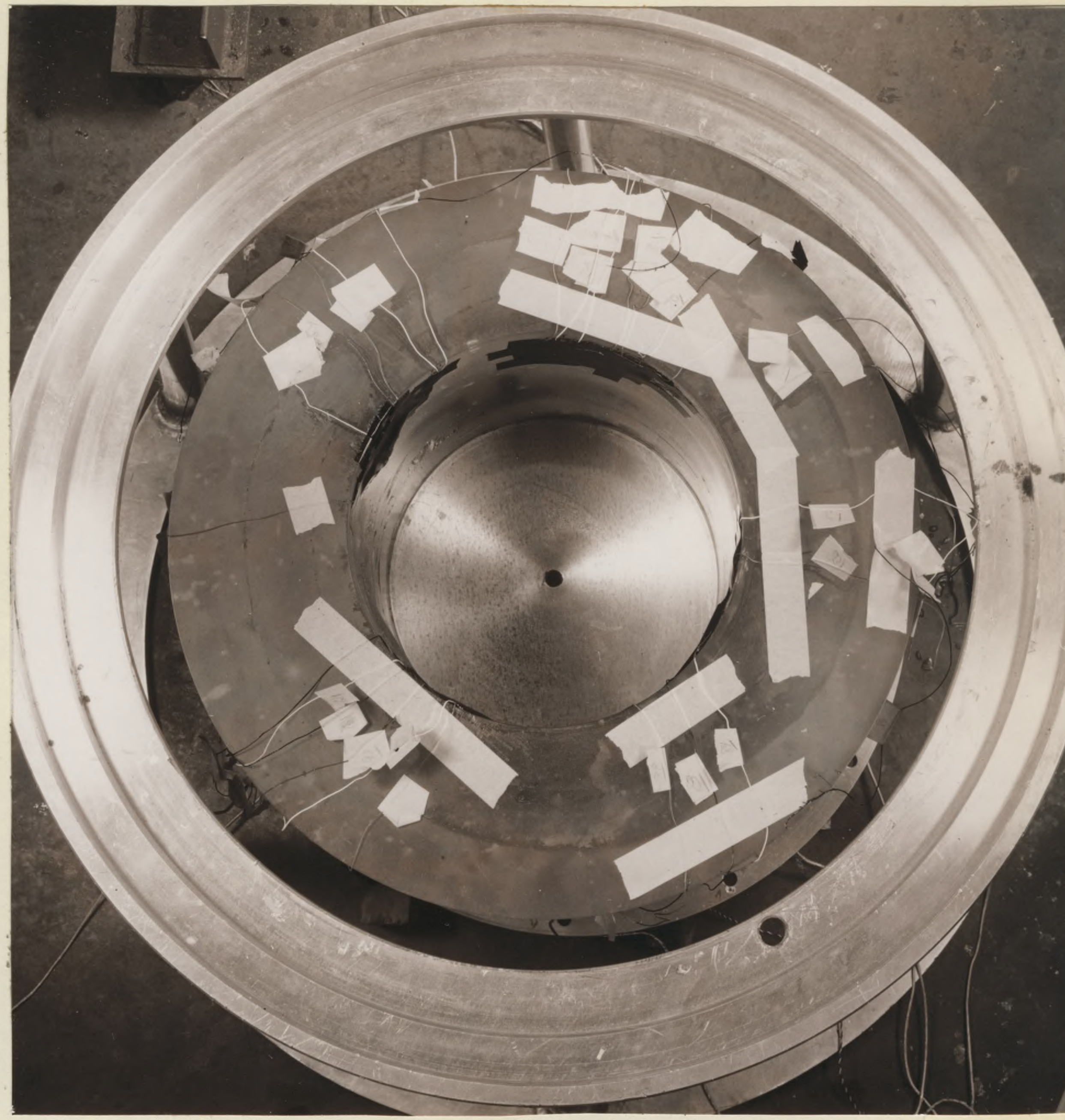

Figure 20. Interior of Model Pressure Vessel

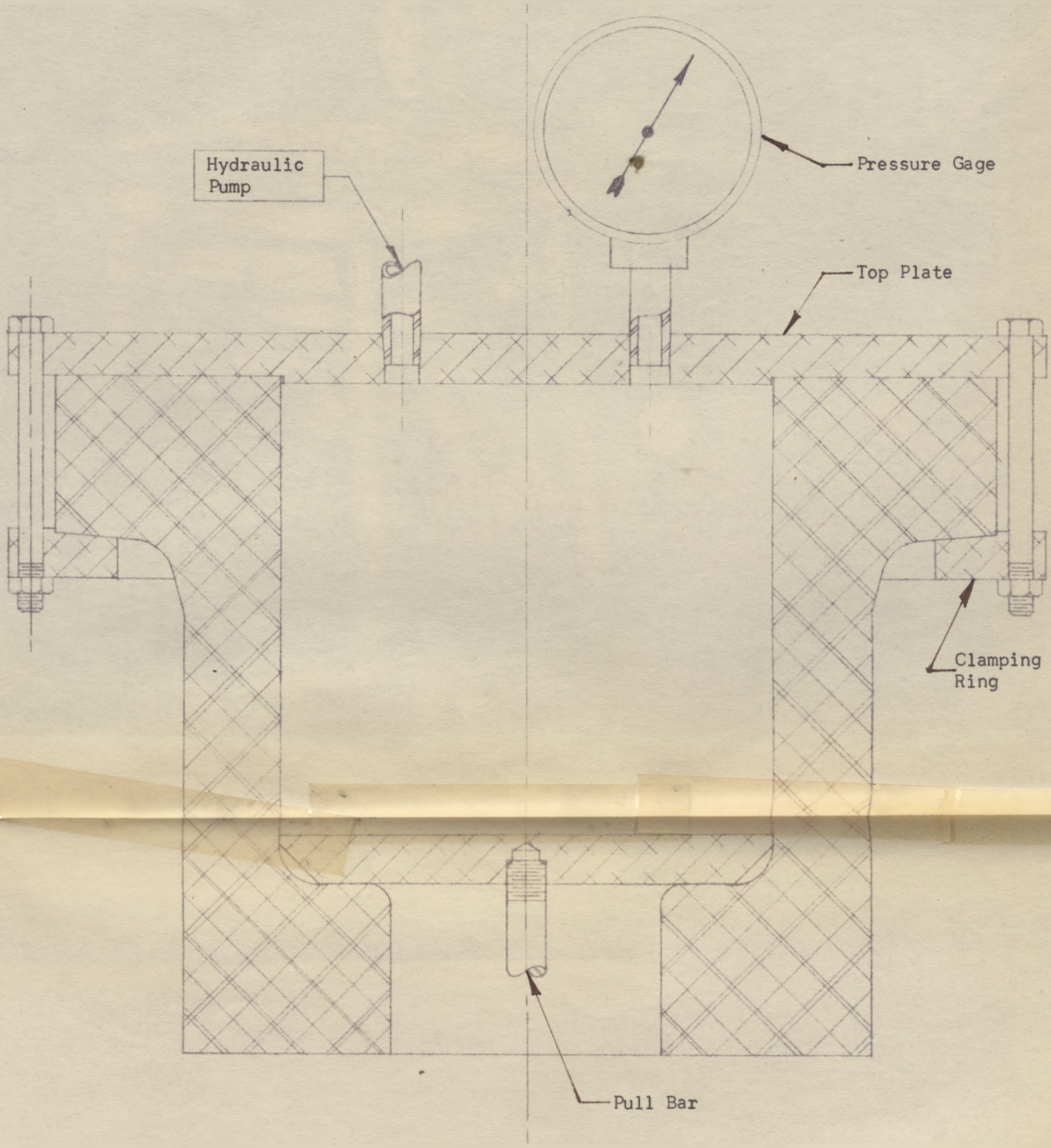

Figure 21. Pressure Test of Thick Wall Vessel

Figure 22. Apparatus for Internal Pressure Test

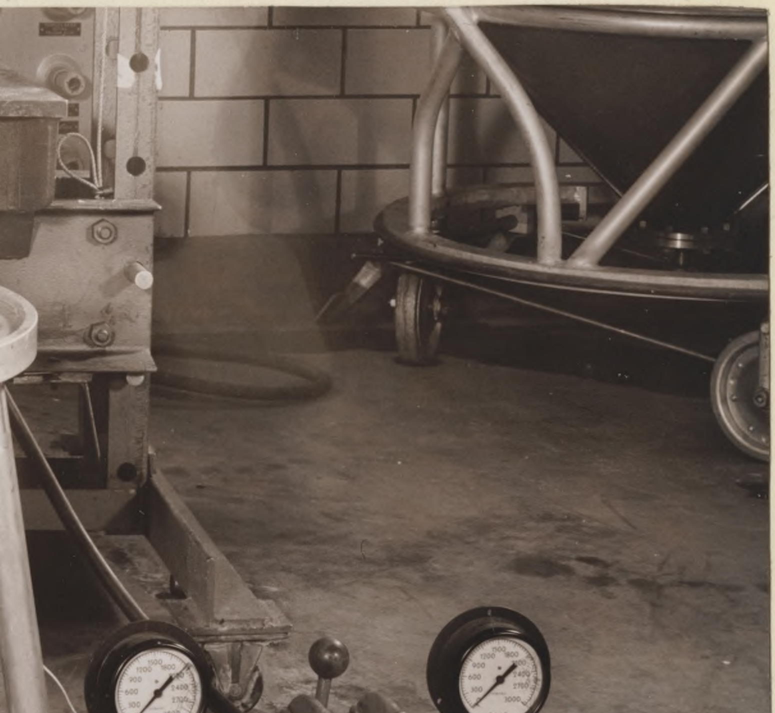
300
600
900
1200
1500
1800
2400
2700
3000
300
600
900
1200
1500
1800
2400
2700
3000

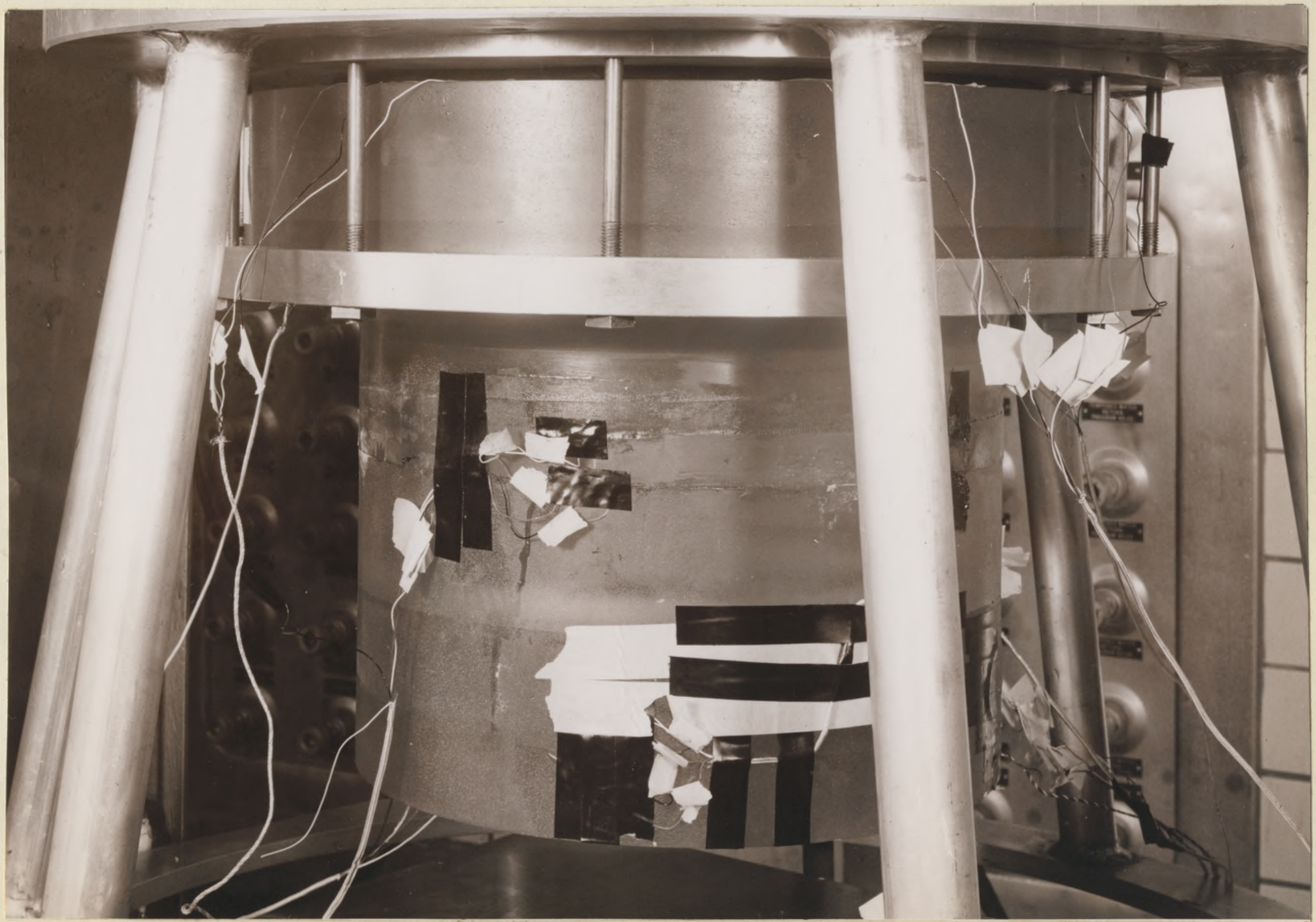

Figure 23. Close-up of Model Suspended in Holding Fixture

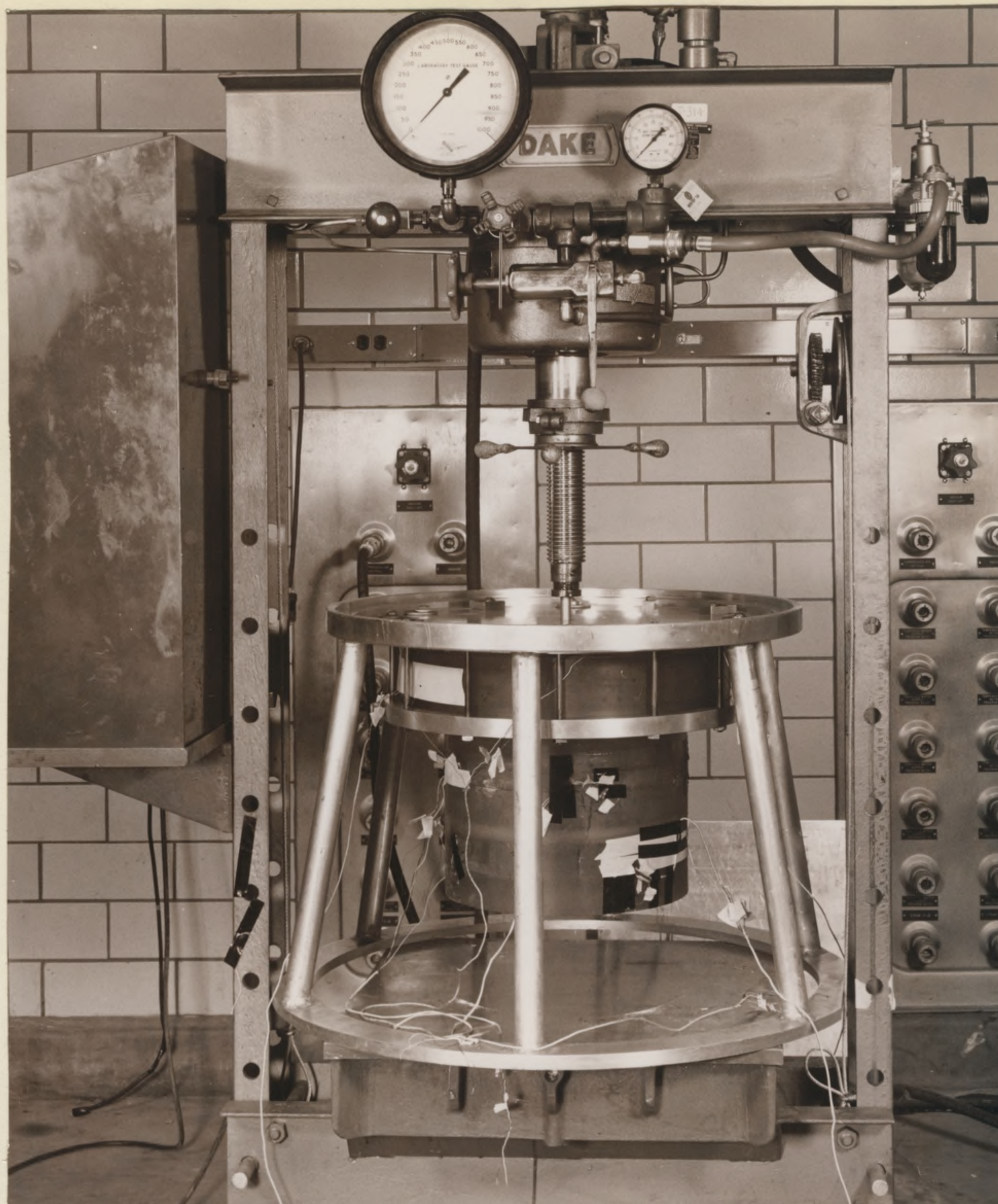

Figure 24. Apparatus for Static Load Test

IX. RESULTS

Gages 1 through 12 were imbedded at the center section of the model. At this location they should be sufficiently far removed from end restraint that their output, particularly the gages which are oriented tangentially, should compare with the theoretical values calculated by convential thick wall pressure vessel formulae.

The following table gives a comparison of experimentally determined and calculated tangential strain values.

Table 2. Comparison of Experimental and Calculated Strain Values

Gage Location	Test Condition	Measured Strain μin/in	Calculated Strain μin/in	Fillet Radius
Inner Radius	90 psi	495	466	3/4
Center of Wall	90 psi	372	374	3/4
Outer Radius	90 psi	280	319	3/4
Inner Radius	85 psi	486	441	1/2
Center of Wall	85 psi	398	354	1/2
Outer Radius	85 psi	342	301	1/2
Inner Radius	35 psi	170	182	1/4
Center of Wall	35 psi	134	146	1/4
Outer Radius	35 psi	115	124	1/4

At locations where there was more than one gage the average of the readings was taken. As might have been predicted, the upper fillet radius had no effect on the strain in the center section.

From the longitudinal gages in the center section a comparison can be made with theory when the model is loaded statically through the lower plate as well as when subjected to internal pressure. The following table gives this comparison.

Table 3. Comparison of Experimental and Calculated Strain Values

Gage Location	Test Condition	Measured Strain μin/in	Calculated Strain μin/in
Inner Radius	4710 lbs	119	106
Center of Wall	4710 lbs	180	106
Outer Radius	4710 lbs	219	106
Inner Radius	5010 lbs	173	113
Center of Wall	5010 lbs	226	113
Outer Radius	5010 lbs	237	113
Inner Radius	90 psi	-89	159
Center of Wall	90 psi	83	159
Outer Radius	90 psi	209	159
Inner Radius	85 psi	-105	150
Center of Wall	85 psi	116	150
Outer Radius	85 psi	275	150
Inner Radius	35 psi	-29	61.7
Center of Wall	35 psi	31	61.7
Outer Radius	35 psi	87	61.7

If these numbers were believed exactly, the only conclusion would be that the model is not in equilibrum. This is clearly impossible. The most plausible explanation is that the entire model is subject to bending due to eccentricities of loading and support. Since only three of the six vertical gages in the center section were active this can not be proven definitely. However, it can be noted that the results of the internal pressure tests more nearly agree with theory then do the results of the static load tests.

From this data it appears that bending stresses are introduced into the walls of the vessel, resulting in higher stresses at the outer surface but lower stresses at the inner surface, in the center section.

Gages 13 through 24 were located behind the lower fillet radius of

the model. Here it is desired to determine the stress concentration factor associated with this 3/4 in radius. If we define the stress concentration factor K_t as the maximum stress measured at a point divided by the calculated stress at the same radius in the center section of the vessel. Then, the stress concentration factor associated with the lower fillet radius is given in table 4.

Table 4. Stress Concentration Factor at Lower Fillet Radius

Test Condition	Measured Strain μin/in	Calculated Strain μin/in	K_t
90 psi	558	159	3.5
85 psi	611	150	4.1
4070 lbs	382	106	3.6

The three factors given actually represent three measurements of the same factor. Actually a value of 3.8 should be used. This compares with a value of 3.5 used in the theoretical investigation. For the last two test conditions the second arm of the rosette was inactive. It was assumed, from data taken from ajacent gages that the strain in the inactive arm would have been essentially zero.This was the case for the readings taken before the gage was broken.

Gages 25 through 44 were located behind the upper fillet radius of the model. Here again, it is desired to determine the stress concentration factor associated with this radius. This was only partially successful. Only 11 of the 20 gages were active at the beginning of the test. The arrangement of these 11 gages was such that few complete rosettes were available. There was no gage located tangentially behind the 3/4 in fillet

radius. Table 5 gives the output of the gages in the upper section under various conditions.

Table 5. Pressure Vessel Strain Readings

Gage No.	3/4 in Radius 90 psi	1/2 in Radius 85 psi	1/4 in Radius 35 psi	1/2 in Radius 4710 lbs	1/4 in Radius 5010 lbs
28	215				
29	240	140		355	
31	240				
32	220	155		0	
33	130	130	5	275	450
35	80				
37	-10	-20	-5	120	100
38	260				
39	30	75	-35	110	130
41	-105	-75	-30	25	-5
42	265			-35	

As can be seen, some of these readings are inconsistant. For example, the output of gage no. 29 is 140 at 85 psi with a 1/2 in fillet radius but it is 240 at 90 psi with a 3/4 in fillet radius. Gage no. 33 has a reading of 450 at 5010 lbs with a 1/4 in fillet radius but only 5 at 35 psi with the same radius. Once again, this may be due to misalignments is loading and support but it can only be concluded that insufficient information was obtained to get a true picture of the stress state in this area.

If the readings of the gages tangent to the 1/2 in and 1/4 in radii are taken during the static load test, stress concentration factors of 4.9 and 5.9 are obtained. This compares with values of 6.5 and 4.5 used in the theoretical investigation.

radius. Table 5 gives the output of the gages in the upper section under various conditions.

Table 5, Pressure Vessel Strain Readings

Gage No.	3/4 in Radius 90 psi	1/2 in Radius 85 psi	1/4 in Radius 35 psi	1/4 in Radius 4710 lbs	1/4 in Radius 5010 lbs
28	215				
29	240	140		[illegible]	
31	240				
32	220	135		0	
33	130	130	5	275	450
35	80				
37	-10	-20	-5	120	[illegible]
38	250				
39	30	75	-35	110	[illegible]
41	-105	-75	-30	[illegible]	[illegible]
42	205			25	

As can be seen, some of these readings are inconsistent. For [illegible] the output of gage no. 29 is 140 at 85 psi with a 1/2 in fillet [illegible] but it is 240 at 90 psi with a 3/4 in fillet radius. Gage no. 33 [illegible] reading of 450 at 5010 lbs with a 1/4 in fillet radius but only [illegible] psi with the same radius. Once again, this may be due to [illegible] in loading and support but it can only be concluded that [illegible] information was obtained to get a true picture of the stress [illegible] this area.

If the readings of the gages tangent to the 1/2 in and 1/4 in [illegible] are taken during the static load tests, stress concentration [illegible] 4.9 and [illegible] are obtained. This compares with values of [illegible] in the theoretical investigation.

X. CONCLUSIONS

It was concluded that the inclusion of a strain element in a plastic model does not significantly alter the stress distribution in the model. Therefore, the method used in this work is well suited to three dimensional stress analysis.

It was concluded that this method is subject to the following sources of error: (1) Non uniformity of gages- Calibration tests on sample gages indicate a possible error in gage factor of ±4%. (2) Nonhomogeneity of the model- The present technique of assembling the model from many pieces lead to the inclusion of some air bubbles which resulted in voids in the wall of the model. The exact error due to this is not known but it is undoubtedly reflected in the discrepency between measured and calculated stress values for the center section of the vessel. The amount of disagreement here was found to be ± 13%. (3) Error in position of the gages- From thick wall pressure vessel theory a difference of 1/32" in the location of a gage at the inner radius of the vessel would result in a 1% difference in stress. (4) Error due to a high stress gradient- Due to the size of the gage the output actually represents the average stress in a volume 1/4" x 3/8" x .012". If the stress gradient is high this average will differ from the maximum stress.

It is concluded that model studies made by this method will be subject to an error of not more than ±10% provided the stress gradient is not too high.

It is concluded that the stress concentration factors associated with the 3/4" lower fillet radius, the 1/2" upper fillet radius, and the 1/4" upper fillet radius are 3.8, 4.9, and 5.9 respectively. However, the reliability of the last two values is in doubt.

It was thought [illegible] cons not significantly [illegible] the method [illegible] analysis.

It was [illegible] entities (1) [illegible] a possible [illegible] present techniques of [illegible] tion of [illegible] exact [illegible] electrons [illegible] section [illegible] (b) [illegible] difference of [illegible] would [illegible] [illegible] [illegible] element [illegible]

It is [illegible] an array [illegible]

It is [illegible] additional [illegible] [illegible]

XI. RECOMMENDATIONS

In view of the anticipated use of the pressure vessel the use of a three inch fillet radius is recommended at both the upper and lower flanges. This will result in the lowest maximum stress and should lead to a longer service life for the vessel.

Since one of the great advantages of this method of experimental stress analysis is that the effect of several different parameters can be investigared with a single model, I recommend that the effect of change in section and the effect of varying both the fillet radius and the cylindrical radius be more thoroughly investigated to give a more nearly complete range of values. This should be most useful in the design of closures for thick wall pressure vessels.

It is felt that Castolite may not be the ideal material for further model work in this field. Its selection for this project was based upon a combination of good photoelastic and mechanical properties. However, now that it has been demonstrated that the imbedding of electrical resistance strain elements in the model has a negligible effect upon the stress distribution, the photoelastic properties of the model material are of only secondary importance. Several resins currently available offer higher mechanical strength and greater ease of casting. It is believed that they also possess the property of bonding to themselves so that a model could be fabricated. The use of these materials should be investigated.

Etched, metal foil gages have recently appeared on the market. They are supplied with a strippable plastic backing. While these gages have a

slightly greater mass than the wire gages used in this work, they still may not disturb the stress distribution in a model. Their use should be investigated since this would greatly simplify the job of constructing the model.

With this new technique, for the first time, three dimensional experimental stress analysis is possible on a model subjected to dynamic forces. Also, by imbedding a small thermocouple with the strain gage, stresses due to temperature gradients can be measured as well as those due to applied forces. Both of these fields are worthy of further investigation.

Consideration should also be given to the use of this method in conjunction with three dimensional photoelasticity since definite, numerical values of strain at points in a tri-axial stress field would greatly simplify the photoelastic analysis.

slightly greater [illegible] gives [illegible] may

not disturb the [illegible] should [illegible]

cated since [illegible] the [illegible]

[illegible] that [illegible]

mental stress analysis [illegible] possible [illegible]

Also, [illegible]

to [illegible]

forces [illegible]

Consideration should [illegible] the [illegible]

ion which [illegible]

of steel [illegible] plots [illegible]

problems [illegible].

XII. LITERATURE CITED

(1) Matzdorff, Roger E., Castable plastics in photoelastic stress analysis. Engineers Thesis, California Institute of Technology. Pasedena, California. 1950.

(2) Frocht, M.M. and Hui Phi., A new cementable material for two and three dimensional photoelastic research. Proceedings of the Society for Experimental Stress Analysis. Vol. XII, No. 1, 55-64. May, 1953.

(3) Loh, Y.C., Internal stress gauges for cementitious materials. Proceedings of the Society for Experimental Stress Analysis. Vol. XI, No. 2, 13-28. 1954.

(4) Dove, Richard C. Strain measurement errors in materials of low modulus. Proceedings of the American Society of Civil Engineers. Vol. 81, Separate No. 691. May, 1955

(5) Dietz, A.G.H. and Campbell, W.H., Bonded wire strain gage techniques for polymethyl methacrylate plastics. Proceedings of the Society for Experimental Stress Analysis. Vol. V, No. 1, 59-62. 1947.

(6) Eney, W.J., Discussion of paper entitled Bonded wire strain gage techniques for polymethyl methacrylate plastics. Proceedings of the Society for Experimental Stress Analysis. Vol. V, No. 1, 63-66. 1947.

(7) Clark, Austin B.J., Static and dynamic calibration of a photoelastic model material, CR-39. N.R.L. report No. 4779, Naval Research Laboratory. Washington, D.C. June 7, 1956.

(1) McCormick, Roger A., [illegible]

Engineers Thesis, California [illegible]

[illegible]

(4) [illegible], Richard [illegible]

Proceedings of the [illegible]

Separate No. 691 [illegible] 1955

(5) [illegible]

(8) Gerard, George and Gilbert, Arthur C., Photothermoelasticity: an exploratory study. Technical report SM 56-11. College of Engineering, Research Division, New York University. University Heights, New York. May, 1956

(9) Murphy, Glenn. Advanced mechanics of materials. pp 114-127. New York, McGraw-Hill Book Co., Inc. 1946.

(10) Peterson, R.E., Stress concentration design factors. p 126. New York, John Wiley & Sons, Inc. 1953.

(11) Perry, C.C. and Lissner, H.R., The strain gage primer. New York, McGraw-Hill Book Co., Inc. 1955.

(12) Lee, G.H., An introduction to experimental stress analysis. pp 114-117, 135-140, 148-223. New York, John Wiley & Sons, Inc. 1950.

(13) Meier, J.H., Strain rosettes. In Hetényi, M., Handbook of experimental stress analysis. pp 407-415. New York, John Wiley & Sons, Inc. 1950.

(14) Dohrenwend, C.O. and Mehaffey, W.R., Electrical-resistance gages and circuit theory. In Hetényi, M., Handbook of experimental stress analysis. pp 170-175. New York, John Wiley & Sons, Inc. 1950.

(8) Gerard, George and [illegible] [illegible] [illegible]
[illegible] [illegible] [illegible]
Research Division, New York University, [illegible]
May, 1956
(9) Murphy, Glenn, Advanced Mechanics of Materials, [illegible]
McGraw-Hill Book Co., Inc., 1946.
(10) Peterson, R.E., Stress Concentration Design Factors, [illegible]
John Wiley & Sons, Inc., 1953.
(11) Perry, C.C. and Lissner, H.R., The Strain Gage Primer, [illegible]
McGraw-Hill Book Co., [illegible]
(12) [illegible] [illegible]
135-140, 129-132. New York: [illegible]
(13) [illegible], Strain Gages. In [illegible]
Stress Analysis, [illegible]
(14) Dohrenwend, C.O. and Mehaffey, [illegible]
[illegible] Handbook of Experimental Stress Analysis, [illegible]
pp. [illegible] [illegible]

XIII. ACKNOWLEDGEMENTS

The author is grateful for the advice, suggestions, and guidance of Dr. Richard C. Dove, Associate Professor of Mechanical Engineering, University of New Mexico, who served as advisor throughout this problem.

Appreciation is expressed to Dr. Fred W. Dubois, and Mr. Edward Casados of the Los Alamos Scientific Laboratory, University of California, for assistance in the design and construction of the plastic model.

Acknowledgement is made to Mr. Edward Sass, and Mr. Arthur Quackenbush for their aid in constructing the apparatus and to Mr. Tom Chandler for help with instrumentation.

The author is [illegible] Dr. Richard C. Dove, [illegible] University of New Mexico, [illegible]

Appreciation is expressed [illegible] of the Los Alamos Scientific Laboratory [illegible] assistance [illegible]

Acknowledged [illegible] of their aid in constructing the [illegible] with instrumentation.

XIV. APPENDIX

Data from evaluation and calibration tests.

Strain readings were taken with a Baldwin portable strain indicator.

Additional reference information is also included.

RESISTANCE OF STRAIN ELEMENTS

Gage no.	Gage length inches	Resistance ohms
1	1/2	119.3
2	1/2	119.4
3	1/2	119.4
4	1/2	119.1
5	1/2	119.3
6	1/2	119.5
7	1/2	118.8
8	1/2	119.5
9	1/2	119.5
10	1/2	119.3
11	1/2	118.6
12	1/2	119.3
13	1/4	119.7
14	1/4	119.8
15	1/4	119.9
16	1/4	120.5
17	1/2	119.3
18	1/2	118.8
19	1/2	118.8
20	1/2	118.4
21	1/2	119.0
22	1/2	119.1
23	1/2	119.0
24	1/2	119.4
25	1/4	120.1
26	1/4	120.4
27	1/4	119.6
28	1/4	120.2
29	1/4	119.9
30	1/4	119.8
31	1/4	120.2
32	1/4	119.8
33	1/4	120.1
34	1/4	119.3
35	1/4	120.5
36	1/4	120.2
37	1/2	119.3
38	1/2	118.3
39	1/2	118.9
40	1/2	118.9
41	1/2	119.4
42	1/2	118.9
43	1/2	118.8
44	1/2	118.3

CALIBRATION BEAM STRAIN READINGS - TENSION

Dial Indicator reading inches	Gage no. 48 microin./in.	Gage no. 34 microin./in.	Gage no. 45 microin./in.	Gage no. 53 microin./in.
.1900	7635	8705	11950	15160
.1800	7860	8880	11990	15250
.1790	7915	8940	12035	15300
.1780	7975	8995	12090	15350
.1770	8035	9053	12150	15400
.1760	8100	9110	12205	15460
.1750	8160	9165	12270	15520
.1760	8090	9110	12215	15470
.1770	8025	9048	12160	15420
.1780	7970	8985	12105	15370
.1790	7905	8925	12050	15320
.1800	7853	8870	12000	15270
.1900	7695	8725	11970	15065
.1800	7870	8915	12235	15195
.1790	7930	8965	12300	15245
.1780	7990	9023	12350	15300
.1770	8050	9080	12410	15365
.1760	8115	9135	12470	15425
.1750	8175	9195	12530	15490
.1760	8100	9140	12475	15435
.1770	8045	9080	12415	15385
.1780	7980	9015	12355	15325
.1790	7920	8955	12300	15280
.1800	7865	8905	12240	15230
.1900	7720	8765	12110	15135

CALIBRATION BEAM STRAIN READINGS - COMPRESSION

Dial Indicator reading inches	Gage no. 48 microin./in.	Gage no. 34 microin./in.	Gage no. 45 microin./in.	Gage no. 53 microin./in.
.1900	7640	8740	12020	15130
.1800	7355	8430	11680	14835
.1790	7295	8375	11620	14775
.1780	7240	8320	11570	14715
.1770	7185	8265	11505	14660
.1760	7130	8205	11450	14610
.1750	7075	8155	11390	14550
.1760	7140	8210	11470	14610
.1770	7200	8275	11533	14670
.1780	7260	8330	11615	14720
.1790	7315	8390	11660	14780
.1800	7370	8440	11715	14840
.1900	7640	8710	12035	15155
.1800	7455	8435	11695	14850
.1790	7405	8380	11640	14795
.1780	7340	8320	11590	14735
.1770	7285	8260	11530	14680
.1760	7225	8205	11465	14630
.1750	7175	8147	11405	14570
.1760	7245	8210	11490	14630
.1770	7300	8275	11555	14700
.1780	7355	8340	11620	14755
.1790	7415	8395	11680	14810
.1800	7465	8450	11755	14870
.1900	7655	8780	12050	15160

CROSS SENSITIVITY CALIBRATION STRAIN READINGS

Load pounds (1)	Gage no. 48 microin./in.	Gage no. 45 microin./in.
0 (2)	6500	15371
10	6502	15377
30	6504	15380
50	6510	15388
70	6517	15393
90	6521	15398
110	6526	15402
130	6530	15410
150	6536	15415
170	6542	15423
190	6548	15425
170	6544	15420
150	6540	15413
130	6535	15410
110	6528	15402
90	6520	15397
70	6518	15390
50	6512	15384
30	6505	15378
10	6500	15373
0	6496	15370

(1) This load was applied over an area of two square inches.

(2) At the zero load condition approximately four pounds of apparatus was on the test specimen.

PRESSURE VESSEL STRAIN READINGS

Gage No.	Zero Reading	30 psi	60 psi	90 psi
1	9800	9750	9723	9690
2	5290	5360	5485	5650
3	10610	10585	10530	10510
4	11890	11990	12075	12240
5	9995	9995	10000	10010
6	5990	6060	6150	6240
7	11560	11560	11575	11595
10	11330	11375	11450	11500
11	9160	9200	9240	9280
12	9930	9990	10025	10110
13	12280	12440	12530	12660
16	13840	13805	13790	13835
20	8205	8195	8190	8260
22	7655	7660	7660	7720
23	3760	3750	3745	3760
24	8820	8830	8830	8870
28	13305	13390	13445	13520
29	11880	12000	12030	12120
31	11540	11660	11690	11780
32	14320	14420	14460	14540
33	12400	12470	12480	12530
35	11800	11895	11850	11880
37	8300	8305	8290	8290
38	13770	13890	13935	14030
39	8360	8390	8385	8390
41	7780	7745	7720	7675
42	16790	16910	16955	17055

Internal Pressure Test

Gage factor setting on strain indicator = 2.0

Gage no. 45 used as compensating resistor

Upper fillet radius = 3/4 in.

PRESSURE VESSEL STRAIN READINGS

Gage No.	Zero Reading	44 psi	85 psi	Zero Reading
2	4570	4700	4900	4570
3	11155	11100	11040	11135
4	10900	11035	11260	10900
6	5210	5320	5485	5210
7	11905	11920	11950	11895
10	10645	10740	10875	10635
11	9630	9685	9790	9620
12	9055	9130	9250	9050
13	11930	12115	12345	11925
20	8530	8465	8485	8470
22	7530	7530	7525	7500
23	4250	4210	4215	4205
24	9100	9050	9065	9040
29	11630	11695	11770	11610
32	14370	14415	14525	14350
33	12030	12090	12160	12010
37	8410	8400	8390	8385
39	7990	8020	8065	7985
41	7800	7760	7725	7770

Internal Pressure Test

Gage factor on strain indicator = 2.0

Gage no. 45 used as compensating resistor

Upper fillet radius = 1/2 in.

PRESSURE VESSEL STRAIN READINGS

Gage No.	Zero Reading	35 psi	Zero Reading (model broken)
3	10880	10845	
4	10885	11005	11060
6	5235	5325	
7	11690	11700	
10	10645	10740	
11	9295	9345	
12	9010	9060	8930
20	8150	8160	8095
23	3080	3060	3095
24	8730	8705	8680
33	11975	11980	12025
37	8335	8330	8380
39	8000	7965	8400
41	7595	7565	7585

Internal Pressure Test

Gage factor setting on strain indicator = 2.0

Gage no. 45 used as compensating resistor

Upper fillet radius = 1/4 in.

PRESSURE VESSEL STRAIN READINGS

Gage No.	Zero Reading	100 lbs
2	5090	5070
3	10690	10680
4	11665	11640
6	5860	5845
7	11620	11600
10	11260	11225
11	9155	9150
12	9870	9830
13	12230	12220
16	11240	11240
20	5455	5460
22	7645	7640
24	6080	6080
28	13255	13260
29	11755	11765
31	11315	11315
32	14285	14285
33	12315	12320
37	8280	8280
38	13690	13680
39	8325	8315

Static Load Test

Gage factor setting on strain indicator = 2.0

Gage no. 45 used as compensating resistor

Upper fillet radius = 3/4 in.

These readings are considered insignificant.

PRESSURE VESSEL STRAIN READINGS

Gage No.	Zero Reading	4710 lbs
2	4510	4565
3	11180	11260
4	10900	10870
6	5150	5170
7	11930	12050
10	10580	10580
11	9625	9775
12	9030	9015
13	11890	12150
20	8480	8430
22	7460	7430
24	9035	9035
29	11750	12105
32	14380	14380
33	12100	12375
37	8415	8535
39	7970	8080
41	7780	7805
42	16430	16395

Static Load Test

Gage factor setting on strain indicator = 2.0

Gage no. 45 used as compensating resistor

Upper fillet radius = 1/2 in.

PRESSURE VESSEL STRAIN READINGS

Gage No.	Zero Reading	2040 lbs	5010 lbs	Zero Reading
2	4550	4550	4580	4520
3	11035	11045	11100	10990
4	10860	10860	10890	10830
6	5170	5160	5170	5140
7	11810	11840	11920	11770
10	10590	10565	10580	10560
11	9385	9410	9520	9360
12	8995	8970	8950	8945
20	8235	8175	8150	8190
23	3140	3135	3140	3095
24	8795	8780	8735	8750
32	14250	14250	14250	14240
33	11685	11850	12135	11670
37	8300	8345	8400	8260
39	7880	7930	8010	7865
41	7655	7655	7650	7615

Static Load Test

Gage factor on strain indicator = 2.0

Gage no. 45 used as compensating resistor

Upper fillet radius = 1/4 in.

PHYSICAL PROPERTIES OF CASTOLITE

Density	1.215 gm/cm^3
Modulus of Elasticity, Compression	6.0 - 6.5 x 10^5 psi
Compressive Yield Point	22,200 psi
Velocity of Sound	1.003 x 10^5 in/sec
Poisson's Ratio	.39
Photoelastic Fringe Value	166 lbs/in - fringe

PROCEDURE FOR PREPARING CASTOLITE

1. Disassemble mold completely
2. Coat all surfaces with Dow-Corning Silicone Mold Release number 7
3. Reassemble Mold
4. Put a second of mold release on inside surfaces
5. Mix Castolite in the proportions of 6 drops cumine hydroperoxide per 120 grams resin - mix thoroughly
6. Let cure at room temperature for a minimum of 24 hours
7. Increase temperature to 200°F at a rate of 4°F per hour

   Hold at 200°F for 8 hours

   Cool at a rate of 2.3°F per hour to room temperature

[illegible]

1. Disassemble [illegible]

2. [illegible] Stillson [illegible]

3. Reassemble [illegible]

4. [illegible]

5. [illegible]

(a) [illegible]

6. [illegible]

7. Increase temperature [illegible]

[illegible]

[illegible]

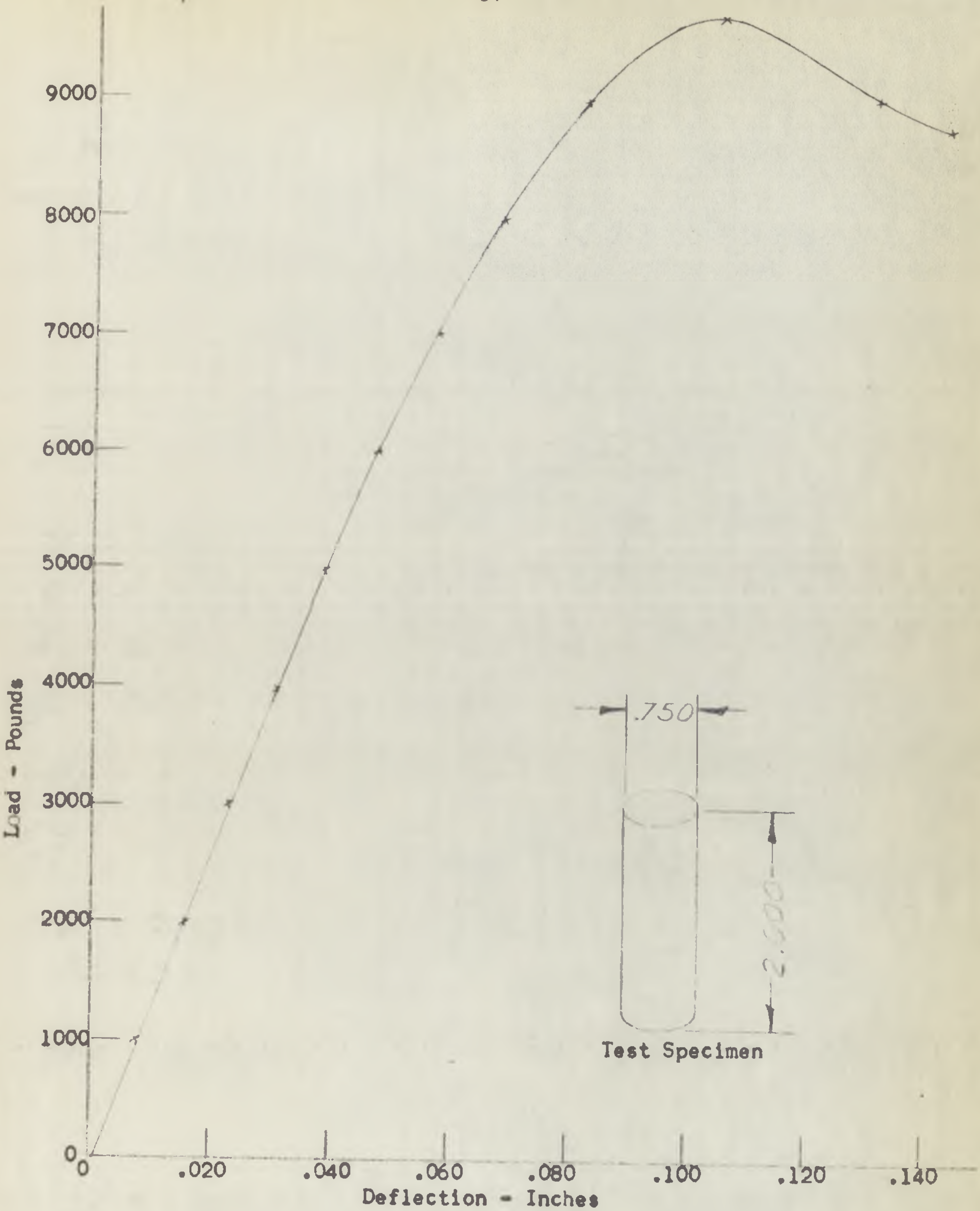

Load - Deflection Curve for Castolite

CALCULATION OF POISSON'S RATIO

Poissons ratio for Castolite was determined from the compressive modulus, the velocity of sound through the material, and the density.

The relationship is: $v = \left[\dfrac{Eg(1-\nu)}{\rho(1+\nu)(1-2\nu)} \right]^{\frac{1}{2}}$

$$\frac{v^2\rho}{Eg} = \frac{1-\nu}{(1+\nu)(1-2\nu)}$$

$v = 1.003 \times 10^5$ IN./SEC.

$\rho = 1.2159 m./Cm.^3 = 1.215 \times .03613 = .04390$ LB./IN.^{3}

$E = 6.5 \times 10^5$ PSI.

$g = 32.2$ FT./SEC.^{2} $= 386.4$ IN./SEC.^{2}

$$\frac{v^2\rho}{Eg} = \frac{(1.003\times10^5)^2 \times .04390}{6.5\times10^5 \times 386.4} = 1.75839 = \frac{1-\nu}{(1+\nu)(1-2\nu)}$$

$$1-\nu = 1.75839 - 1.75839\nu - 3.51678\nu^2$$

$$.75839 - .75839\nu - 3.51678\nu^2 = 0$$

$$\nu = \frac{.75839 \pm \sqrt{.575155 + 1.066836}}{1.51678}$$

$$\nu = \frac{.59262}{1.51678} = .39$$